DEVELOPMENT OF A NANOMETRIC MACHINING CENTER FOR ULTRAPRECISION MANUFACTURING

A Thesis
Presented to
The Academic Faculty

By

Daniel Cox

In Partial Fulfillment
Of the Requirements for the Degree
Master of Science in Mechanical Engineering

Georgia Institute of Technology

May, 2005

DEVELOPMENT OF A NANOMETRIC MACHINING CENTER FOR ULTRAPRECISION MANUFACTURING

Approved by:

Dr. Steven Liang, Advisor
Woodruff School of Mechanical Engineering
Georgia Institute of Technology

Dr. Thomas Kurfress
Woodruff School of Mechanical Engineering
Georgia Institute of Technology

Dr. Shreyes Melkote
Woodruff School of Mechanical Engineering
Georgia Institute of Technology

Date Approved: January 2005

To the one who got me in, helped me stay, and allowed me to finish – my Father in Heaven. Thanks!

Acknowledgements

I would thank my advisor, Dr. Steven Liang for all his direction and expert insight which he has shared with me. In addition I would like to express my gratitude to Precision Machinery Research & Development Center, without whose sponsorship this project would not have been possible. I wish to thank my parents who have continually worked to foster in me a love of learning and encouraged my investigative qualities. Also I want to thank my friends here at Tech who have made this an unforgettable experience, particularly all the Navs and the men of the Pirate House.

Contents

Acknowledgements **iv**

List of Tables **vii**

List of Figures **viii**

List of Symbols **x**

Summary **xi**

1 Introduction **1**

1.1 Literature Survey 4

1.2 Research Approach 8

2 Stage One **10**

2.1 Experimental Setup 10

2.2 Experimental Results 11

2.2.1 One-Dimensional Linear Trajectory Tests 12

2.2.2 Two-Dimensional Circular Trajectory Tests 14

2.2.3 Two-Dimensional Arch Trajectory Tests 17

2.2.4 Three-Dimensional Sculptured Surface Trajectory Tests 18

3 Stage Two **20**

3.1 Experimental Setup 20

3.2 Experimental Results 31

3.2.1 One-Dimensional Linear Trajectory Tests 31

3.2.2 Two-Dimensional Circular Trajectory Tests 32

3.2.3 Three-Dimensional Feature Tests 35

4 Theoretical Model **38**

4.1 Basic Force Model 38

4.2 Maximum Cutting Conditions 39

4.3 Force Measurement 40

Conclusion **54**

A Frame Design **56**

B Frame Schematics **59**

References **63**

List of Tables

3.1 Options for the machine frame 27

4.1 Range of test conditions 42

List of Figures

2.1 Stage one setup 11
2.2 Machined straightness error 12
2.3 Machined wall profile 13
2.4 Machined circle 14
2.5 Circle following error 15
2.6 Circle error tests - 50 & 75 micron 16
2.7 Circle error tests - 50 & 75 micron 17
2.8 Machined arch 17
2.9 Error trends in arch tests 18
2.10 Machined surface 19

3.1 Stage two setup 21
3.2 HPT Spindle-Unit 23
3.3 100μm end mill 25
3.4 Machine frame CAD model 28
3.5 Digital video camera 30
3.6 Miniature dynamometer 31
3.7 Straightness error trends 32
3.8 Straightness error comparison - 5μm d.o.c. 33
3.9 Straightness error comparison - 20μm d.o.c. 33
3.10 Circle following errors 34
3.11 Comparison of circle following errors 34
3.12 Micro hemisphere 35
3.13 Micro bolt 36
3.14 Micro gear 37
3.15 Microscope view of a micro gear 37

4.1 Theoretical force curve 39
4.2 Maximum cutting conditions 40
4.3 Maximum cutting conditions 41
4.4 Measured forces 43
4.5 Measured forces 44
4.6 Measured forces 45
4.7 Measured forces 46
4.8 Measured forces 47
4.9 Force comparison 48
4.10 Measured forces 49
4.11 Measured forces 50
4.12 Measured forces 51
4.13 Measured forces 52
4.14 Measured forces 53

A.1 Finite element model 56
A.2 Theoretical frame stiffness curves 58

List of Symbols

MRR	material removal rate
d	depth of cut
a	width of cut
a_1	exit length
a_2	entry length
v_f	feed rate
s_z	feed
u_c	specific cutting energy
k	corner angle
D	tool diameter
R_a	Average surface rougness

Summary

The demand for reduced-size components and devices is pervasive throughout industrial and commerical sectors. This drive to reduce the achievable size of parts and features has furthered the developmen of processes and tools capable of micro scale fabrication. In particular, one of the directions this field has taken is in scaling down traditional machine tools.

Being a relatively young area of manufacturing, the area of miniaturized machining is still developing and a significant portion of work remains yet to be done. As a thorough understanding of this area is still developing, experimental tests play a significant role furthering this process.

Therefore the direction of this project has been to explore this field using a predominantly experimental approach. The aim of it being to realize a miniaturized machine tool capable of fabricating features and even parts on the micro scale. Additionally the machine should be controlled as a standard milling machine and also be capable of generating free form three dimensional parts. In parallel to developing a machine tool, the project has also been directed at examining the machine's capabilities through a range of tests.

For creating such a machine tool, the process was carried out in a two stages. Each stage involved a miniaturized machine tool at a different level. The first machine tool produced primarily served as a proof of concept structure. By performing a range of tests on this machine, it allowed for useful insights be to gained for developing the subsequent stage along with establishing some base performance characteristics which were also used for subsequent comparisons.

The primary contributions made in this research include: the development of a miniaturized machine, the completion of experiments that map out the machine's capabilities, and theoretical calculations which further define these limits.

Chapter 1

Introduction

Definition and Motivation

Miniaturization is continually driven forward by the demand for reduction in part and product size, both in commercial and industrial sectors. Specific fields that have provided much of the primary motivation include semiconductors, information appliances, consumer electronics, aerospace, and biomedical products and systems. This demand pushes manufacturing forward to develop the ability to reliably create smaller parts. In turn, this has led to the development of new machines and techniques capable of micro scale machining.

Beginning with a definition, micro machining is a branch of manufacturing where the tolerances, features, and even part sizes are on the micro scale. It is an emerging technology where new developments are incorporates into an established area of manufacturing. This combination results in processes or machines in which the domain of work preformed is on the order of 500 - 0.5μm.

Micro metal cutting in particular is being further developed because of its unique advantages over other micro fabrication techniques. Generally, micro fabrication involves the use of: (1) mechanical solid tools for cutting, abrasion, or chemical-mechanical material removal actions; (2) high energy beams such as UV optical, ion beam, e-beam and X-ray, etc.; and (3) scanning probes such as STM, AFM, magnetic, thermal, chemical-reactive probes, etc. as noted by Corbett [1]. Among them, the use of mechanical solid cutting tools fills a niche for industry applications where flexibility, accuracy, and part finish is of great importance. Most of the energy beam techniques

are based on photolithography or scanning probe methods which are based on scanning tunnelling are restricted in the selection of workpiece materials, the possible geometry of features, and the high cost of equipment capital investment.

Photolithography processes employ may be divided into bulk micromachining or surface micromachining (other methods, such as LIGA, may be seen as derivatives or combinations of these two) [2]. In etching techniques, the resulting features will be strongly influenced by the crystal structure of the material or the directional characteristics of the etching process used. Surface micromachining creates features through successive layer deposition of varying materials. Shaping material by layering techniques are usually limited to geometries that can be closely approximated by successive extrusions of two dimensional patterns. In each case, neither of these processes have the ability to create free-form three dimensional features. These techniques typically carry with them several material limitations as well. They are primarily used upon silicon, silicon based compounds, or materials that have been bonded to silicon wafers. In particular, regarding depositing and patterning metals, current techniques rarely use ferrous materials. Further, typical additive techniques such as sputtering, evaporation, or chemical vapor deposition, atomically separate the materials being applied. This does not allow the metal to maintain any treatment properties such as cold working or heat treatment. On the other hand, solid-tool-based processes are not restricted by these factors and they can create one-of-a-kind parts of extremely fine resolutions. In the interest of mass production, these parts can be used as the molds or dies for subsequent casting or injection molding.

Given these advantages of metal cutting, this possibility has already begun to be explored. Within this area, there are two methods used to preform micro machining: retrofitting standard machines with high-precision parts appropriate for small scale cutting, and developing new miniaturized machine tools where the entire machine tools is several orders of magnitude smaller than traditional machines. Though the first option is more easily realized, the second affords the possibility of far better performance along with significant economic benefits. This option is now becoming possible because of new developments in producing high precision components. For example, milling tools with small tip diameters were not available in 1996 [3]. As T. Schaller noted in a report published in 1999 [4], the minimum diameter for commercially available metal end mills at that time was 150μm.

For mechanical solid tool machining, the overall size of machine tools is an underlying factor to the achievable resolution, precision, and overall effectiveness of the processes. In comparison to macro-sized traditional machine tools, systems of miniaturized volume size have a number of inherent and unparalleled advantages including: (a) the increase of thermal resistance due to the reduced heat source intensity and the machine tool volume involved in thermal deformation; (b) the increase of static stiffness resulting from the shortening of structural overhangs; (c) the increase of dynamic stability by virtue of the higher structural resonance frequency for smaller machine size/weight; (d) the lowering of machine cost, thereby allowing the use of more expensive and better quality construction materials; and (e) the increased efficiency in resource utilization in terms of floor space and power consumption.

Technology Issues

Miniaturized manufacturing heavily draws upon the field of conventional manufacturing. However, there are several unique elements in this area, specifically regarding machine frame rigidity, thermal rigidity, contamination, and tool life.

The fundamental issues of manufacturing processes still persist in micro machining, yet the scale has a large impact upon which issues remain significant. For example, basic contamination can be a far more serious issue as the size of dust and dirt particles are not far form that of the features being machine. Such contamination on the tool or clamping device could interfere with the overall accuracy.

Miniaturized cutting tools have shown themselves to behave differently than traditional machine tools. They are often subject to premature tool failure and unpredictable tool life [5]. The issue of tool wear compared to tool breakage is also much different [6] as tools tend to fail from breaking more frequently than they do from excessive wear.

Another very practical issue is that of observing the cutting process. When cutting tools smaller than 0.1mm in diameter are used, it becomes extremely difficult to see the tool. It is very important to accurately know the height at which the tool touches the workpiece as this will significantly influence the accuracy of the cutting depth. This task requires more precision than is possible with human vision. Additionally, observing the tool-workpiece interaction is also very important. For such small tools,

it is possible for them to break during a cutting operation without any visible changes.

1.1 Literature Survey

Around the world, a number of governmental level laboratories such as NIST (U.S.), AIST (Japan), RIKEN (Japan) and academic institutions, as noted in Okazaki *et al*, Lu and Yoneyama, and Vogler *et al* [7], [8],& [9] among others, have actively engaged in the research of microscale machine tools. Of the work done, there have emerged two main approaches in machining at the micro-scale: retrofitting standard machines with high-precision parts and developing new miniaturized machine tools where the entire machine tools is several orders of magnitude smaller than traditional machines. Though the first option is more easily realized, the second affords the possibility of far better performance along with significant economic benefits regarding required space and power consumption. This option is now becoming possible because of new developments in producing high precision components. Following are several summaries of several projects conducted in the field of micromachining.

Miniature Cutting Tools

Several have begun to explore the possibility of designing a machine tool to accommodate a miniature cutting tool. In the mid 1990s a study of the fabrication and testing of micro cutting tools was report by M. Vasile *et al* [3]. The approach of this project was to create microscale features by using miniaturized cutting tools. The micro tools were fabricated by focused ion beam (FIB) machining. Initially, the micro tools were simply scaled down versions of macroscale tools. However, milling with these micro tools was unsuccessful and the traditional tool geometry was replaced by a simpler one. The next iteration of tools used had a cross-sectional shape of a circle with a pair of flats cut into its sides. The diameter of the tools was 23μm, and these tools were used to machine micro trenches in polymethyl methacrylate (PMMA). The spindle used was a commercial microdrill, and the workpiece was moved by a stepper-motor driven stage. The setup was successful in creating two-dimensional geometries such as trenches with surface roughness values less than one micron. Thus this project demonstrated the realization of micro tools and successful machining of

micro features in a soft material like PMMA.

The applications of such work have been presented by C.R. Friedrich [10]. When fabricating micro trenches measuring 23 x 60 x 1500 μm^3, the machining time is extremely large (over three hours). Therefore this micromachining process would not be suitable for direct mass production. Rather it could be used for creating templates such as molds or masks. It could also be useful in the development applications where concept structure is required.

Th. Schaller *et al* [4] described a similar project where micro grooves were cut in a much harder material. Some of the machined grooves had widths as small as 50μm. To create these high precision features, they used micro-scale end mills. These were produced by grinding tungsten carbide rods with diamond impregnated wheels. A wide variety of tool sizes was produced ranging in diameter from 35-120μm. Several difficulties were present in this process as around fifty percent of the tools broke during grinding. In addition, the tool geometry varied a by $\pm$5μm due to the grinding conditions.

The test bed was a commercially available high-precision milling machine fitted with these micro tools. Both brass and stainless steel were used as work piece materials. In the experiments involving steel, 100μm diameter tools were the smallest ones used. In addition burrs formed along the side walls of grooves milled in the steel. These burrs ranged in size from a few microns to over 50μm. Several burr removal methods were suggested and then successfully implemented. Some such techniques include diamond milling, electrochemical polishing, and coating with cyanacrylate.

Miniaturized Machines

An even more novel approach to using miniature tools it to simply miniaturize the entire machine tool. One of the initial steps toward micro cutting by using a miniaturized machine tool was presented by Z. Lu *et al* [8]. The approach undertaken in this project was to reduce the size of a standard machine tool while proportionately reducing the achievable accuracy. As a result, a micro lathe was created and tested. This device had overall dimensions less than 20cm and was composed of a commercially available micro stepping table, DC spindle, and a diamond probe for a cutting tool. The cutting process was observed with an optical microscope.

The lathe was successful in producing miniaturized parts such as a small-sized screw with a diameter of about 120μm. The surface roughness observed from several experiments was under 1μm, which is comparable to conventional precision lathes. Thus the physical size of the machine tools was reduced, though the accuracy was only slightly improved upon.

Miniaturized machine tools have been used in projects aimed at creating microfactories. E. Kussul *et al* [11] presented a survey of two prototype microfactories where the overall size was less than 200 x 200 x 200mm^3 for each design. These prototype microfactories had the ability to perform turning, milling, drilling and grinding operations. This project used an iterative approach where the secondary prototype was built in order to eliminate several drawbacks of the first one while reducing the overall machine size and increasing the accuracy. These microfactories were driven by stepper motors which were controlled by a PC and were attached through gear boxes.

As part of the survey of these prototype machines, they present some theoretical models that show the benefits of miniaturization. Looking at deformations caused by vibrations and thermal changes, they show how these effects are reduced as the primary dimensions decrease. These findings are based upon first-order analytical approximations, but not empirical data.

A primary issue this project addressed was the cost of microfactories. The authors purposed to create a microfactory with extremely low cost, with each of the individual components costing less than one hundred dollars. Such a low cost approach provides extra motivation, yet it prohibited the use of high precision components. The average tolerance errors were around 20μm, and the range of achievable features only went down to 50μm.

A meso-scale machine tool (mMT) was presented by M. Vogler *et al* [9]. The approach taken in this project is to realize a machine tool capable of producing high precision features through size reduction of the machine. In order to compensate for the size reduction, high speed spindles and high resolution positioning tables were used.

The miniature machine tool was tested with air-turbine spindles capable of extremely high speeds (150,000 - 320,000rpm). These were used with two different

positioning systems, one based upon voice-coil drives and the other using piezoelectric motion. The range of tool sizes selected for milling operations was 250-500μm which allowed for reasonable cutting speeds to be achieved. However, this also had a strong bearing on the minimum feature size possible. In a series of circle tests, the smallest circle diameter cut was 0.8mm.

The machine tool was used to machine aluminum and was able to achieve a surface roughness of 0.27μm. The three-dimensional capabilities of the machine were demonstrated curved surface profiles.

In a similar project, W. Lin *et al* [12] presented a study on the development and testing of a reduced-size combination grinding and milling machine which was specifically designed for micro-fabrication. The overall dimensions of the machine were 560x580x650mm^3 and the weight was less than 120kg. The positioning system had a resolution of 0.2μm and was able to mill channels with a width of around 150μm. This project is an example of how medium scale machines may be used with small tools to created features on the micro scale.

Theoretical Models

Work has also been done specifically in the area of tool geometry for micro machining, such as that presented by Fang *et al* [6]. This study examines five tool shapes (conventional 2-fluted, straight and tapered body triangle shaped, and straight and tapered body D-shaped) using both theoretical models and experimental data. The theoretical analysis consisted of an FEA preformed to determine the relative stiffness of the tools and the predicted chipping and breaking forces. Experimental tests used tools with 200μm diameter tips and were conducted for a range of feeds and speeds. The conclusion from both of these considerations was that tapered body tools are preferable for micromachining tools.

Similarly, W. Bao *et al* [13] presented a cutting force model specifically for micro-end-milling. In the proposed model, the chip thickness is calculated based off of the trajectory of the tool tip. The outcome is a slightly more involved method for determining the cutting forces, yet the results of the model have better agreement with the experimental tests detailed in the study. These tests were conducted with tools ranging form 125μm to over 3mm in diameter. These were used in commercial

CNC mills with work pieces of steel and aluminum. The average error between the measured cutting force and the traditional cutting force model was around 15%, while it was about 10% for the proposed model.

In addition to studies preformed upon micro tools, N. Mishima [14] presented an analysis of machine frames for miniaturized machine tools. This paper details an optimization scheme for positioning accuracy of machine tool structures. Specifically, it examined and compared four major frame configurations for vertical milling machines with three axes. The analysis is based upon an analytical model.

The recommendations from the analysis suggest that the vertical stage be incorporated into the spindle overhang. However this style would only have a slight advantage over others. The model also suggested that overall size has a strong influence on machine performance. Specifically, it projected that smaller frames would perform better, with an optimal size being around $1/10^{th}$ that of a standard machine.

Within the area of micromachining, W. Wang *et al* [15] presented a study on the influences of surface roughness. The analysis used a primarily experimental approach with a carefully planned out design of experiment. The experimental setup was comprised of an air-pressure spindle with maximum speed of 120,000rpm and a high precision 3-axis stage driven by stepper motors. Workpiece materials included brass and plastic. The tools used ranged in size from 200-1000μm. After conducting extensive experimental tests, the range of surface roughness values found varied from 2-15μm.

Although these values are fairly high, this did not obstruct the primary objective of the project. From the data, they were able to identify and characterize some factors that influence surface finish which are unique to micro machining. For example tool diameter and the spindle speed were identified as significant influences upon surface roughness. The conclusion reached is that for a better surface finish quality a small feed rate, medium cutting speed and a small diameter tool are needed.

1.2 Research Approach

The goal of this project is to create a miniaturized micro machining center capable of producing features on the micro. That is, this project aims at realizing a fully operational vertical machining center that is miniaturized.

Previous experiments have shown that it is possible to create basic two-dimensional geometries such as channels and wall on the small scale 100-10μm yet none have demonstrated a machine tool that has the capacity to produce truly three dimensional parts. Along with realizing an actual machining center, the setup will be evaluated. This testing of the machine tool will itself layout a series of meaningful benchmarks for micro milling machines.

A secondary objective for the project includes the realization of a tool failure model that will predict critical cutting conditions. This model will map out several of the practical limitations of the machining center that will define a usability range. This model will be based upon a theoretical cutting force model and will additionally be validated with empirical data. Since the model will be theoretical, it can be extended to a range of conditions much greater than the specific tests described herein.

Metal cutting at the micron level has not been investigated as thoroughly as macro and meso scale machining. Even today, there are several areas which are still not well understood. As such, experiments play a key role in moving towards a more better understanding of this branch of manufacturing.

A primary component of this project will be experimentation. It will be exploratory approach towards understanding cutting trends at the micro level and developing a micro machining tool.

The machine tool development will be conducted in two stages. The first will be primarily concerned with developing a proof of concept design, which will be used to gain a basic understanding of the issues present at the microscale and how they could be overcome. The second stage is fully realizing the design and operation of a miniaturized CNC milling machine. The design is based upon results from the first stage and also thorough analysis of the machine. For example, computer models, such as the one of the machine frame shown in the figure below, played an integral part in developing an analytical understanding of miniaturization effects in machine frames.

The specific qualities projected for the machine tool include size: $<0.1\text{mm}^3$, weight: <30kg, minimum resolution: <1μm, and minimum feature size: micro-scale.

Chapter 2

Stage One

2.1 Experimental Setup

A concept miniaturized vertical machining center was assembled and is shown in Figure 2.1. This machine tool is composed of five subparts: machine frame, spindle, cutting tool, positioner, and imaging device. The main purpose of this setup was to provide a base performance level which could be used to evaluate later design iterations. As such, several components were chosen primarily for their availability rather than their functionality. The following paragraphs each give a brief description one of these components.

The machine frame is a gantry structure which consists of four corner pillars which support a solid base and top. The outer dimensions of the frame define the size of the machine tool as 350mm, 240mm, and 320mm (length, depth, and height respectively). The material selected for the frame is Invar 36 steel alloy. The material is chosen for its low thermal expansion coefficient, which reduces thermal deformation effects.

The imaging device is a simple hand held digital video camera. Lens ranging from 50x to 200x may be attached to magnify the image. The camera is directly mounted on the frame and is primarily used to set the tool height and to observe the cutting process.

At the top of the figure, the spindle is shown. The spindle shaft rotates on hybrid bearings (ceramic balls fitted in a steel race). The drive of the spindle is a brushless DC motor with maximum rotational speed of 60,000rpm. Models up to 120,000rpm are available with the same mechanical assembly. The high rotational speed is very

Figure 2.1: Proof of concept vertical milling machine.

important as it provides significantly increases the surface cutting speed which in turn lowers the overall chip load. This is necessary because the tool is extremely delicate due to its very small size. The runout of the spindle is rated to less than 1μm.

The cutting tools used are uncoated solid carbide end milling cutters. They flutes are formed by precision grinding with diamond impregnated wheels. They come in the form of two-fluted, square-end or ball-end tools that have tip diameters ranging from 10∼200μm with a shank diameter of $1/8^{th}$ inch in general.

The servo positioning stage, functioning as a machining table, consists of a work holder and a 4-axis system driven by direct drive linear motor with crossed roller bearings. The linear positioning resolution is 10nm by 10nm by 4nm in the X, Y, and Z directions and a rotational positioning resolution of 0.045 s^{-1}. The work volume as defined by the ranges of axes travel are 4mm by 25mm by 25mm in the height, feed, and cross feed.

2.2 Experimental Results

The microscale machine tool's performance characteristics were evaluated through a series of machining tests. These experiments only involved the three linear axes of the positioning table without using the rotational axis. This was done so that

the results of these tests could be compared to other three-axis systems, as this is the most common configuration found in miniaturized machine tools [14]. All of the experiments were preformed on prismatic blocks of aluminum 2024-T4 with 2-flute square-end solid carbide cutters. In order to appropriately judge the machine tool, three classes of test were performed: one dimensional cuts (linear trajectory), 2-D cuts (circular and arch trajectories), and 3-D cuts (sculptured surface).

2.2.1 One-Dimensional Linear Trajectory Tests

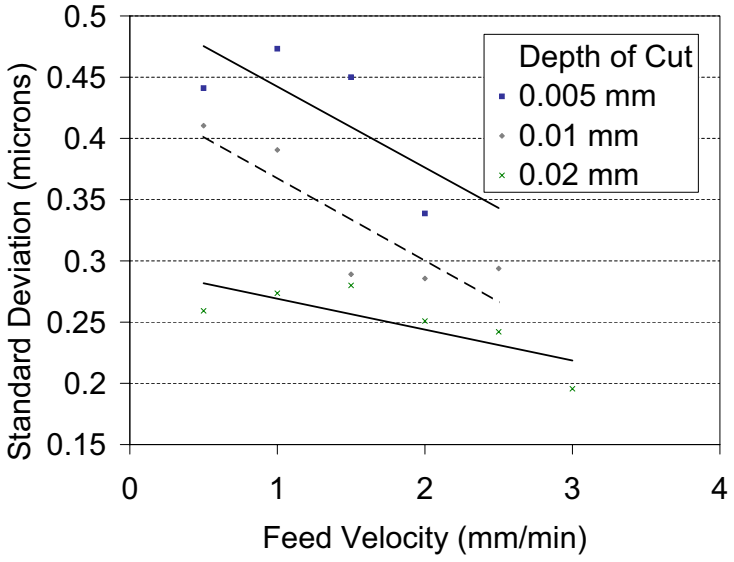

Figure 2.2: Standard deviation verses feed rate and depth-of-cut

For these tests, a series of linear workpiece segments were machined to examine the straightness and finish varied under different machining parameters. In these tests the machine tool simply slot milled a straight line. The cuts were 1-mm long and were done in one pass. In these tests, tools of 100μm in diameter were used at the constant spindle speed of 60,000rpm with a constant axial depth of cut of 100μm (the whole width of the tool was cutting). The feed velocities ranged from 0.5 to 3.0mm/min and depths of cut from 5 to 20μm. The machined surfaces were measured with a white-light inferometer to create three dimensional surface profiles. Data points corresponding to the vertical walls of machined slots were then extracted from these profiles. The straightness error of these sides walls, and hence the tool

path's error, was defined in terms of the standard deviation between the profile and the theoretical straight feed line.

Figure 2.2 shows the machined section straightness error as functions of feed velocity and depth of cut. Higher feed velocity and greater depth of cut generally lead to a better straightness accuracy, as would be expected due to higher stability. Overall, the straightness errors remain between 0.2μm to 0.5μm. At this level the measurement noise becomes relatively pronounced, therefore the variation within each of the trends is rather visible.

Another set of segments were end milled in an up milling configuration. For these cuts, the axial depth of cut was kept constant at 50μm while varying the feed velocity and radial depth of cut. Figure 2.3 graphs the surface finish in terms of R_a as functions of feed velocity and depth of cut. Finish between 0.5μm and 1.5μm are generally achievable within the range of parameters tested. Irregularities in the data mask any correlation between the surface finish and the depth of cut and feed velocity. The use of conventional surface roughness measurement to conduct and extract accurate surface finish data from a microscale tool poses a challenge due to the fact that the measurements were performed over a very limited area (two hundredths of a square millimeter), which contributes to the variances in the R_a values

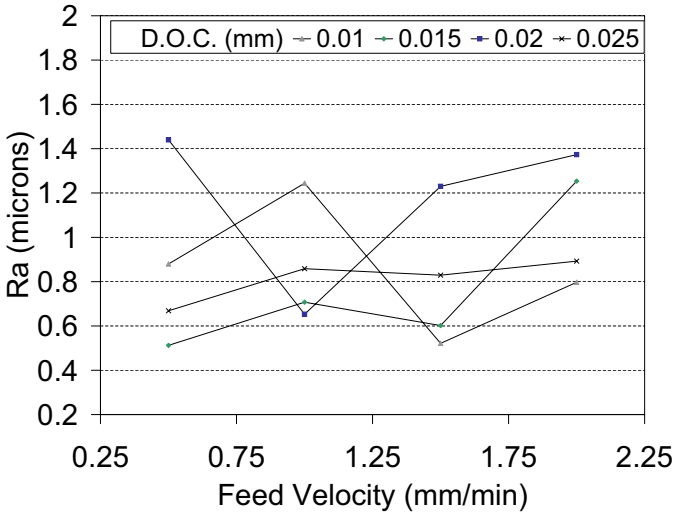

Figure 2.3: Machined wall profile for a series of radial depths-of-cut

2.2.2 Two-Dimensional Circular Trajectory Tests

A 100μm diameter tool was used to follow circular trajectories of 50μm to 600μm inner radius in a single pass. The purpose of this test was to explore the form accuracy achievable in a standard trajectory pattern along the X-Y plane without height variation. Spindle speed of 60,000rpm, feed velocity of 0.5mm/min, and depth of cut of 20μm were applied. The machined surface was analyzed with a white-light interferometer to obtain a three dimensional surface plot. This data was then analyzed with the program MetroloGT to compare the shape of the machined circle with a perfect circle. An example of a 600μm radius cut is shown in Figure 2.4 with the image inverted vertically from a recess to an extrusion pattern.

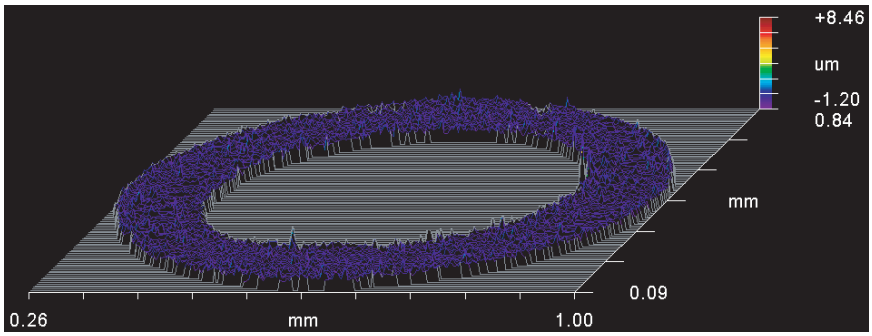

Figure 2.4: Surface roughness plot of the recessed floor of a machined circle

In following a circular path in the X Y plane, the machined region leaves two vertical walls – one referred to as the outside circle and the other as the inside circle – with their radius difference being the tool diameter. It was noticed that the machined outside circle was near perfectly-round but the inside circle shows a distorted pattern. For cuts with smaller circular radius, the inside circle exhibits a greater deviation from the theoretical trajectory. This roundness error caused the average radii of both the inside and outside borders to be smaller than their theoretical values. The percent error between the actual and theoretical values is charted for a series of circles in Figure 2.5. The data has been fit to second order polynomials showing the trends.

In addition to examining the effect of radius size on the form error, the effect of axial depth-of-cut in circular trajectory following was considered in a similar way. Two series of circles were milled, each performed in one pass with a fixed inner circle

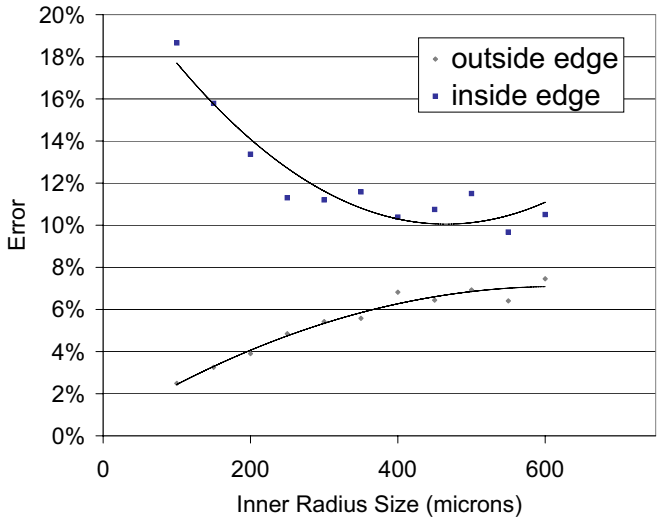

Figure 2.5: Percent error versus inner circle radius for circle following tests

radius. The first series, which had an inner radius of 50μm, is charted in Figure 2.6. The second had an inner radius of 75μm and the error is graphed in Figure 2.7. It is seen that the percentage form error associated with the outer edge is fairly negligible throughout, that is, the outer geometry remains fairly circular in all cases. On the other hand, with a smaller radius, the form error associated with the inner edge increases in its percentage value but decreases in its absolute value. It is very interesting to note that the circular trajectory following motion leads to a near-perfect circle on the outside and a distorted circle on the inside. Equally interesting is that the inside circle becomes more distorted as the circular trajectory used is smaller in its radius.

Although the physical mechanisms contributing to this behavior have not been fully understood, a qualitative model can be pictured to explain the formation of a distorted inside circle from the point of view of average cutting forces. Along a curved machining trajectory with certain curvature, the portion of cut outside of the cutter center line inevitably assumes greater cutting forces than the portion of cut inside. This is a result of the greater material removal rate, thus the greater chip load and greater cutting forces on the outside portion. It can be shown kinematically that the ratio of each material removal rate (MRR), averaged over the entire outside portion and the inside portion, is

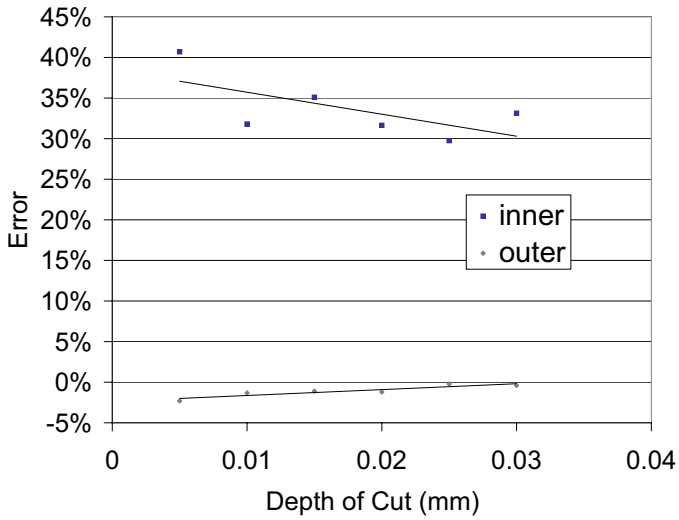

Figure 2.6: Percent error versus inner circle radius for 50μm circle tests

$$r_m = \frac{MRR_{outside}}{MRR_{inside}} = \frac{2R + r}{2R - r} \tag{2.1}$$

where r is the cutter radius and R is the radius of curvature of the machining trajectory. The ratio r_m determines the extent of cutting force unbalance between the outside and inside portions when the machining trajectory is not a straight line. A greater force unbalance would lead to the cutting tool being deflected more toward the inside portion, thereby creating a reduced inner edge radius. Since the milling force variation is periodic, the deflection actually takes on the manner of oscillatory vibration. Depending upon the stiffness variation between the X and Y directions, the vibration motion can have a different magnitude leading to the overall distorted shape of the machined feature on the inside circle. With a larger axial depth of cut providing a higher system rigidity, the vibration motion is suppressed more in its magnitude. In the case of a near-straight trajectory with greater R, this ratio r_m approaches unity indicating less force unbalance and a lower form error. This model explains in part why the form distortion of the inside circle is sensitive to the axial depth of cut and the radius of the machining trajectory curvature.

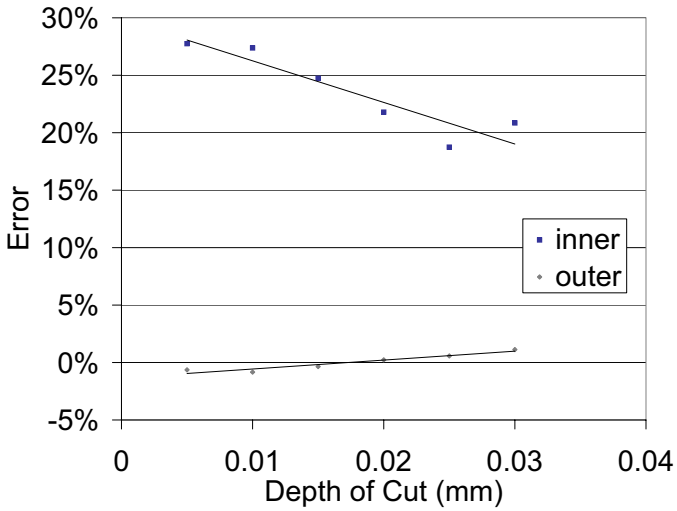

Figure 2.7: Percent error versus inner circle radius for 75µm circle tests

2.2.3 Two-Dimensional Arch Trajectory Tests

Tests were conducted to create a slightly more complicated feature with the height varied along the feed direction in the form of a rising arch with no motion in the cross feed direction. The set of tests serves to explore the achievable part form compliance along the X-Z plane, as opposed to the X-Y plane accuracy discussed previously.

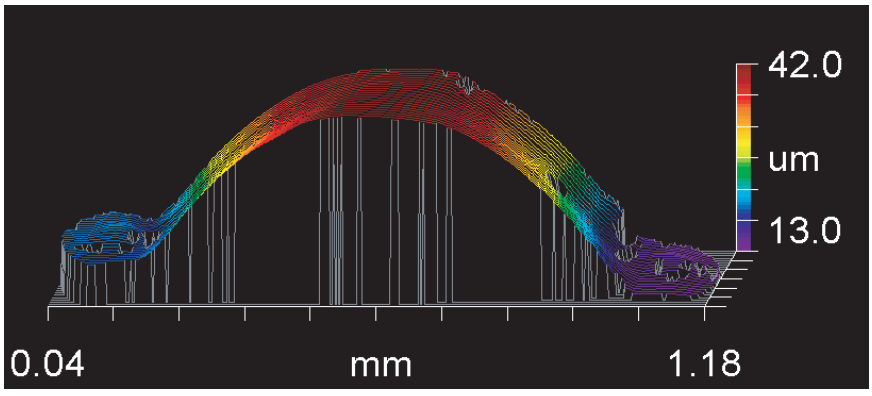

Figure 2.8: Surface roughness plot of a machined arch

Figure 2.8 shows the example of a constant-radius vertical arch generated with 100µm tool running at 60,000rpm machining an aluminum workpiece with a feed

velocity of 0.5mm/min. The machined arch profile is fitted to a regression circle, which has a radius that can be compared to the theoretically programmed arch radius value. The form accuracy in this set of tests is defined as the deviation of machined arch radius from the theoretical value. Figure 2.9 shows a basic series of arch data in the context of form accuracy. Although there is no strong correlation between the error and the size of the arch, this chart does show that the arch form error is limited to 5% over the range of arch sizes tested.

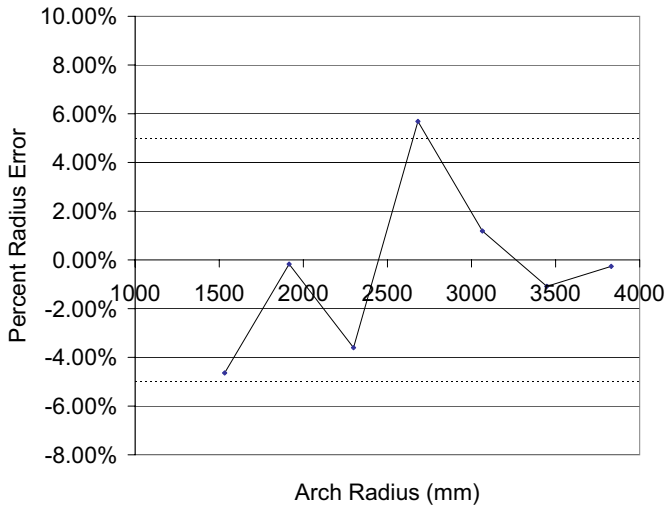

Figure 2.9: Data series of percent errors verses arch radius

2.2.4 Three-Dimensional Sculptured Surface Trajectory Tests

The ability to generate truly 3-dimensional part features gives mechanical solid tool machining and edge over other processes of micro machining which use layer-based approaches. In this set of tests, a 3-D geometric CAD model of sculptured surface, as shown in Figure 2.10a, with length and width of 1mm by 1.5mm respectively, is converted into CNC command files for machining on the microscale vertical machine center. The tool path simulation is shown in Figure 2.10b, and Figure 2.10c shows the resulting surface generated with a 100μm flat end mill over a total machining time of 25 minutes. The general profile features on the machined part follow those on the geometry model rather well over the portions where the slope gradients are mild. For

the portions with sharper variations, such as those around the front-and-back ridge locations, greater challenges in the part geometry conformance are found.

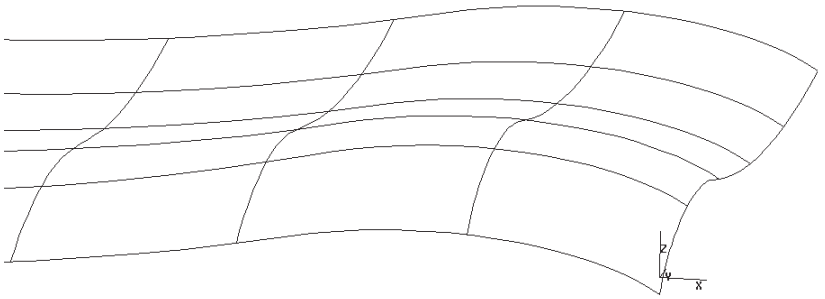

(a)

(b)

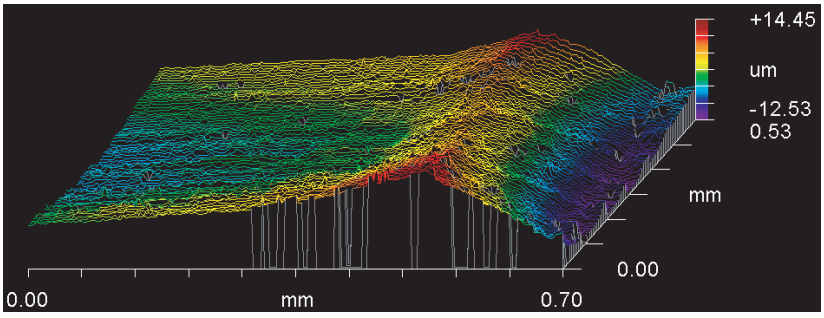

(c)

Figure 2.10: Process of machining a surface contour: (a) computer generated model, (b) simulation of the machined surface, (c) roughness plot of the machined contour

Chapter 3

Stage Two

3.1 Experimental Setup

For the second stage a great deal of time was spent on selecting the appropriate components. The following section details the requirements of each component and the final decision. Again, the micro machine tool may be seen as five main subparts. These being a spindle, cutting tool, positioning stage, frame, and inspection device. Figure 3.1 shows these components.

Motor and Spindle Unit

Requirements: A motor used in a micro machining application must be able to run at a very high speed while maintaining a low runout. The high speed allows parts to be machined in a reasonable amount of time. As the cutting tool itself is extremely small and sensitive, the depth of cut and feedrate are kept relatively low. Yet the material removal rate is balanced out by the spindle speed. The low runout is necessary because of its direct effect upon the minimum possible feature size. Running at high spindle speeds also introduces two other potential problems, heat production and shorter spindle life.

Available Technologies: An important consideration for high speed spindles is the type of bear used. The two main catagories of bearings (contact and non-contact) will both be examined.

Non-contact bearings use a fluid or electric fields to support the shaft within a spindle. Liquid is used as the supporting fluid in hydrostatic and hydrodynamic

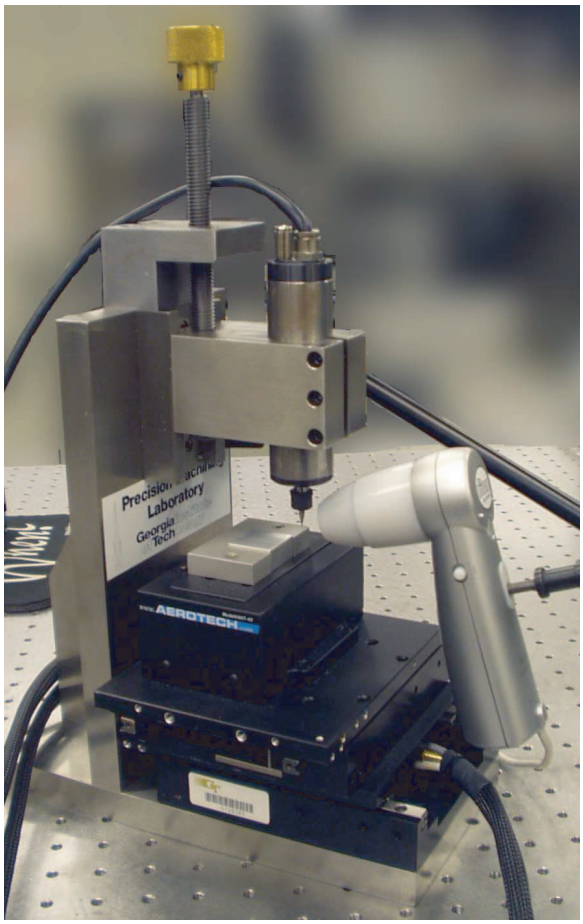

Figure 3.1: The second stage of the miniaturized vertical milling machine

bearings. These spindles have the advantage of the fluid pressure tending to hold the spindle in the center of the shaft giving them a lower runout. However they are usually very inefficient because of the resistance from the viscous forces.

In air bearings, the shaft rests upon a pressurized gas (usually air). These spindles are typically characterized by a low runout. They also tend to have a lower stiffness, making them more appropriate for lighter loads. Air bearing systems also require several pieces of external equipment such as a motor, pump, filter, hoses, etc.

Magnetic bearings employ a series of precisely controlled electric fields to levitate the spindle shaft. These systems have a great deal of versatility as the speed, stiffness, and even rotational error can all be dynamically controlled. This permits these spindles to have very good performance characteristics. Magnetic bearing systems tend to have sizable external controllers and carry a very large initial cost as well.

Contact bearings employ an intermediate rotating solid element that rolls or slides between the shaft and the housing. A primary factor that affects performance is the method used for lubricating the intermediate element.

Of the possible lubrication methods typical ones use either grease or oil. Of these, the most common method is to lubricate the bearing with grease by a adding it to the space between the balls and the race. This grease is permanently sealed within the bearings. As a result, such bearings require minimal maintenance and a fairly low initial and operating cost.

Oil lubrication on the other hand relies upon an oil flow cycled through the bearing. There are two main oil delivery methods, oil jet and oil mist. The oil jet method uses a high pressure stream to deliver oil directly into the bearing race. The oil is then channelled through cooling and filtering stages. Similarly, the oil mist method combines the oil from a reservoir with compressed air and sprays the oil droplets into the bearing. Next it collected, filtered, and pumped back into a reservoir. Because of the mechanisms required to reclaim, filter, store, and pressurize the oil, these systems have a significant amount of external components and equipment. Compared with sealed grease systems, they also require far more upkeep. These systems also require very careful control as the oil must be delivered at the proper rate to effectively cool and lubricate the bearing.

An additional consideration for types of spindles is the tool clamping mechanism. Commercially available clamping systems include collets, hydraulic clamping, and shrink fits. These methods can all provide a significant deal of clamping force and precision, both of which are necessary for high speed, low runout systems. Of these types, hydraulic clamping systems are the most complicated and tend to require a larger amount of hardware at the tool-spindle interface. They typically have a lower max RPM as the spindle must also rotate the pressurized fluid used for clamping the tool along with the pipes, channels, etc used in these tool clamps. Shrink fitting systems are extremely simple and provide a very high clamping force. The primary draw back of these systems is the higher cost. Collets provide reasonable overall features (balance concentricity, run-out, holding force) and are one of the lowest cost options as well.

Part Selection: The best intersection of these options was found to be the HPT

Figure 3.2: HPT spindle-unit FS 33-60

spindle-unit FS 33-60 (see Figure 3.2). This is a compound spindle-motor unit employing a small sized DC motor with hybrid bears and sealed grease lubrication. As this motor-spindle unit is relatively small (O.D. = 1.3in), it is able to run at sufficiently high RPMs. The runout of the spindle is kept low as the spindle is precision made and uses hybrid bearings. These bearings employ ceramic balls placed in a metal race. The ceramic balls are much stiffer than traditional steel bearings and therefore deflect much less at higher speeds. This both reduces the runout and the friction between the balls and race, thus the bearings run cooler and with less wear than standard all metal bearings. The spindle employs a collet system for holding the tool.

Cutting Tools

Requirements: The tools used for cutting the metal have two main requirements. They must have a small tip diameter and they must have a high toughness. The tip size directly correlates to allowable minimum feature size, hence it is desirable to have extremely small tool tip diameters (<< 1mm). The toughness is needed to protect the tool against failure due to shock. And particularly for micro scale tools, breaking due to shock is more of an issue than tool wear [6]. Frequently micro tools are subject to premature failure or unpredictable tool life [5], thus it is extremely important to choose tools where the fabrication process and the base materials are all extremely high in quality.

Available Technologies: For high speed machining, there are many options for cutting tools materials. Ones commonly employed in high speed machining include carbide, CERMETS, CBN, and PCB.

Carbide is one of the most common tool materials used in high speed machining. These tools frequently employ a coating such as titanium nitride (TiN), titanium carbon nitride (TiCN), and titanium aluminum nitride (TiAlN). These materials typically increase tool life by decreasing overall wear rates. They also increase the thickness of the tool.

Ceramics and ceramic metals tend to maintain good high temperature hardness. However, tools fabricated from these materials tend to cost more as they are used less frequently than other materials such as carbide.

Other materials which exhibit high resistance to wear include polycrystalline diamond (PCD), which is used for non-ferrous materials, and cubic boron nitride (CBN), which is used for steels. However compared to carbide, they have a lower toughness. These materials are typically made as inserts, and miniature tools made from them tend to be very expensive or are not available.

Within the domain of micro-sized tools, there are several different tool geometries available. Using WEDM, micro tools with tip geometries such as cylinders, extruded polygons, and cones have been reliably created for several years now [16]. Several such commercially available micro tools were examined in a study of tool breakage by Fang *et al.* [6]. This study examined two-fluted end-mills along with non-traditional triangle-based (δ-type) and semi-circle based (D-type). The δ and the D-type geometries were both examined with a straight body and a tapered body. The FEM analysis preformed ruled out the straight body style for δ- and D-types due to their low rigidity. It also showed how the tapered styles of these two types have a rigidity roughly one order of magnitude greater. From a strictly structural point of view, these tools have the most favorable characteristics for micromachining. However the drawback of a tapered tool is its lack of ability to create vertical sidewalls which are necessary for many applications.

Part Selection: To meet these requirements, a solid carbide end mill was selected (see Figure 3.3). These carbide tools are capable of milling plastics, aluminum, copper, and even hardened steel. They are made of ultra-fine grain carbon carbide which allows the tool tips to be produced down to the micro scale. The fine grain size not only allows tools as small as ten microns to be fabricated, but it also makes for stronger tools. The cutters are two-fluted mills with square ends. Tools with straight bodies were selected as they have more a larger range of possible part geometries.

Figure 3.3: 100µm solid carbide end mill with a square end

These tools are available with tips as small as ten microns in diameter. They are fabricated by precision grinding using diamond impregnated wheels. The tools are uncoated to achieve the highest possible resistance to shock. As tool coatings usually protect against wear, they are not as important for these micro tools where the chances of failure due to shock is more common than excessive tool wear.

Positioning Table

Requirements: The positioning table has some of the highest requirements as the largest part of the machining accuracy rests upon its capabilities. Therefore the table must have both an extremely low resolution and a very low repeatability error to ensure both accuracy and precision. In addition to having a high degree of control over the position of the table, the velocity must also be able to be carefully controlled.
Available Technologies: Typical ultra-precision positioning systems typically use one of two mechanisms, piezoelectric drives or linear electric motors. Each of these methods have demonstrated the ability to achieve submicron positioning accuracy [17], [18].

Since piezoelectric materials exhibit a coupling between internal dielectric polarization and strain [2], they may be caused to change shape resulting from an applied voltage. By using multiple layers of piezoelectric materials in series, basic actuation

may be created. There are many such devices commercially available. It is possible to make devices in the form of multi-axis positioning systems with minimum positioning resolutions under a nanometer.

The induced strain is very small, and this permits a high degree of accuracy, yet it also results in a very small range of motion. Typical commercially available systems do not allow for a large range of motion (>0.5mm) [17].

In addition, since the piezoelectric effect is an on/off phenomenon, positioners based upon these materials are more capable of handling step inputs rather than ramp inputs. Thus such devices are not as suited for following velocity commands. Another drawback of these systems is their relatively low working load. This is also due to the small size of the piezoelectric elements used.

Linear motors systems rely upon high precision motors controlled with feedback from extremely precise sensors. Though these systems tend to have higher minimum resolutions than piezoelectric ones, they do offer a much greater range of travel [18]. In addition, since these systems are motor controlled, they may be driven at variable speeds.

However linear motor positioning systems are typically much larger than piezoelectric based ones. For motor driven positioners, each stage requires its own set of rails and motors. These components themselves are also macro-scale devices, unlike the microscale layers found in piezoelectric tables, which contributes to the greater size.

Part Selection: These stringent demands are best met in the Aerotech three-axis linear motor table controlled by A3200 Full-NMotion controller. This positioning table is composed of two identical horizontal stages and one vertical stage. The stages use linear brushless servo DC motors and high resolution non-contact feedback sensors. The total resolution of the positioning table is 5nm x 5nm x 2nm with an extremely low repeatability of 20nm. The ability to position accurately at this scale is key to producing submicron features.

The table also allows the velocity to be accurately controlled. As each stage is controlled by DC motors, the speed of the motors and hence the stage, may be controlled as a simple function of voltage. This, coupled with the high resolution sensors, allows the speed of each stage to be specified to a high degree of accuracy. This is a very important feature as milling is usually based upon constant velocity

movement, while devices such as a piezoelectric positioning table use an on or off effect as the method of locomotion.

The NView software is also capable of interpreting CNC code, either through conversational or standard G-code commands. This allows the micro machine to be used as a standard CNC milling machine where it can be coupled with a CNC code generator to produce parts based upon complex computer generated models.

Machine Frame

Requirements: The requirements of the machine frame primarily involve its stiffness. In addition to the static stiffness and the dynamic properties of the frame being important, the thermal stiffness is also very significant. Anytime a machining operation takes an extended period of time, the fame itself may change size slightly during process as a result of temperature changes in the room or heat produced from the motor and spindle. In many cases, thermally generated errors are small enough that they can even be neglected, but for micro machining applications they become far more significant.

Available Technologies: There are two main concerns regarding machine frames, the frame material and the frame design. The choice of material can be made by comparing basic physical properties of different metals with a comparison such as the one shown in Table 3.1. This table shows some sample values for potential materials. The catagories of metals shown here are low carbon steel, high carbon steel, high-strength aluminum, and specialty iron alloy. This data is from this taken from ASM metal handbooks [19, 20, 21].

Table 3.1: Comparison of material properties for potential frame materials

Material	1020 Steel	1080 Steel	Al 7075-T6	Invar 36
Rockwell Hardness (B)	68	99	87	70
Tensile Strength, Ultimate (MPa)	420	1050	572	448
Tensile Strength, Yield (MPa)	350	783	503	276
Modulus of Elasticity (GPa)	205	205	71.7	141
Density (kg/m^3)	7870	7850	2810	8050
Thermal Conductivity (W/m-K)	51.9	47.7	130	10.15

Part Selection: Both issues of static and thermal stiffness are addressed by fabricating the frame out of Invar 36. This nickel-iron alloy was primarily chosen because of it's relative low coefficient of thermal expansion. The actual stresses applied to the structure will likely be fairly low and each of these materials would provide adequate strength. Thus thermal expansion coefficients became the main determining factor.

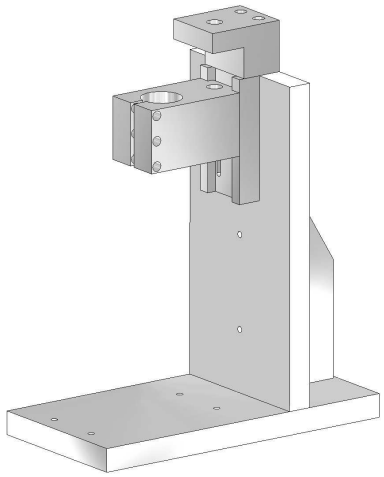

Figure 3.4: A CAD model of the machine frame

The dynamic properties of the frame can be influenced by the specific dimensions of the individual parts of the frame. Using computer modelling, these parts have been sized accordingly to give the table a higher natural frequency and static stiffness. The design criteria for the frame was heavily based upon the work done by H. W. Park as detailed by Cox *et al* [22]. This study on miniaturization of machine tool frames examined the advantages of reducing the size of the primary dimensions of a machine frame in terms of dynamic characteristics, static stiffness, and thermal stiffness. The core results of this analysis may be summarized by noting that both thermal and static stiffnesses along with the natural frequency will all improve with decreasing overall frame size. The frame was therefore designed to be as small as possible while properly accommodating the positioning table and spindle. For a more complete example of this work refer to Appendix A.

A model of the machine frame is shown in Figure 3.4. The total volume of the machine frame is 320 x 260 x 130mm^3 (height, length, and width respectively). See Appendix B for detailed schematics of the frame.

Inspection System

Requirements: Even though the inspection system does not affect the machining process, it is a very important part of the machine tool setup. With micro sized end mills, observing tool-workpiece interactions without magnification is not possible. An inspection system is required to properly set the vertical height offset of the tool and to determine whether the tool is still cutting and that the tip did not break off. For an inspection system to be applicable to micro machining, it must be a small sized device itself so that it does not interfere with the spindle or table.

Available Technologies: In general there are three types of observation devices: pure optical magnification, video capture systems, and complete vision systems. Plain optical systems are the simplest and cheapest option of these three. It simply involves a set of leses connected to an eyepiece. The primary drawback of such systems is that it is difficult to observe the cutting process while simultaneously operating the machine's computer interface.

Video capture systems are basically a optical system with a camera attached instead of the eyepiece. The camera may be either analog or digital, which can be especially useful as the output may be displayed on the same computer as the machine interface. The most applicable type of devices are hand-held microscopes. These consist of a palm sized body with a crook-neck end containing the lenses and camera. These cameras have ranges from 5-1000x magnification, though lenses above 500x have a zero contact length thus would interfere with observing metal cutting. Their small size is especially desirable for use with miniaturized machining.

Complete vision systems have the widest range of capabilities of the three technologies. These systems usually involve a very sophisticated video capture unit combined with computer measurement and analysis. The imaging unit may take lenses that magnify from zero to four thousand times. Even at the upper end of this range, these units may still maintain a working distance of over 1cm. The units may include complex mirror and lens arrays which allow for multiple lighting and inspection angles. The measurement portion of these systems allows for precise dimensional measurements and shape or feature recognition. These systems tend to cost over an order of magnitude greater than simple video capture ones.

Part Selection: An appropriate solution to these requirements is a hand-help video

microscope. The selected systems is the Scalar Proscope, a video camera with a high zoom objective (see Figure 3.5). Using various detachable lenses and a CCD sensor, the camera produces clear and adequately magnified views of the tool and workpiece. The device can record continuous video or take still shots. It can use lenses that magnify from 10-250x while maintaining focal lengths between 0.25 and 1.0cm.

Figure 3.5: The Scalar Proscope digital video camera shown with a 50x lens

Additional Equipment

Isolation Table - The entire machine tool system must be protected from vibrations. It is important to damp vibrations around the machine tool, both high frequency vibrations that may be produced by the machine and also lower external vibrations that may be caused by the surrounding environment.

Placing the micro machine setup upon an isolation table will handle these issues. The table chose for the micro machine is a Newport VH - Workstation. The table is configured with a set of four high damping isolation modules which specifically dissipate high frequency vibrations. The table is also capable of revealing itself to within a quarter millimeter and has natural frequencies (horizontal and vertical) in the low hertz range [23]. Damping out higher frequencies is very important as the spindle will produce a large harmonic at its rotational frequency which will be on the order of 1000Hz.

Dynamometer - The miniaturized machine tool was also equipped with a small-sized dynamometer for measuring cutting forces. The Kistler 9256C2 MiniDyn (see Figure 3.6) was found to be a suitable choice. This device passed the weight requirement of being less than 4kg (the maximum load of the vertical stage of the positioning

Figure 3.6: The Kistler miniature dynamometer

table). The outer dimensions were also reasonably small, 100 x 100 x 25mm^2, which still allowed for an acceptable amount of clearance between the tool and workpiece after it had been mounted on positioning table. This dynamometer also has a very low measurement threshold (<0.002N) [24] which is critical for detecting the cutting forces produced by micro-sized end mills.

3.2 Experimental Results

The experiments conducted for the second stage were similar to those completed in the first stage to allow for more opportunities for comparison. These included straight line tests, circle following and three dimensional feature generation. All of these tests were performed on workpieces made of 7075-T6 grade Aluminum. The end mills used were 100μm in diameter, and the spindle speed was set at 60,000rpm.

3.2.1 One-Dimensional Linear Trajectory Tests

In these experiments, a series of slot milling operations were preformed to evaluate the straightness errors. The parameters of feed speed and depth-of-cut were varied to gauge the achievable accuracy. The actual measurment was again performed with a white-light inferometer and the output was numerically analyzed in terms of standard deviation from a straight line. Two of the data series are shown in Figure 3.7 where the depth-of-cut was varied from 5 - 20μm and the feed speed from 0.5 - 3.0mm/min. As previously noted, some of the variance is due to the limited resolution of the inferomenter. The significance of these results is that the measured errors are all around or even under one-half a micron.

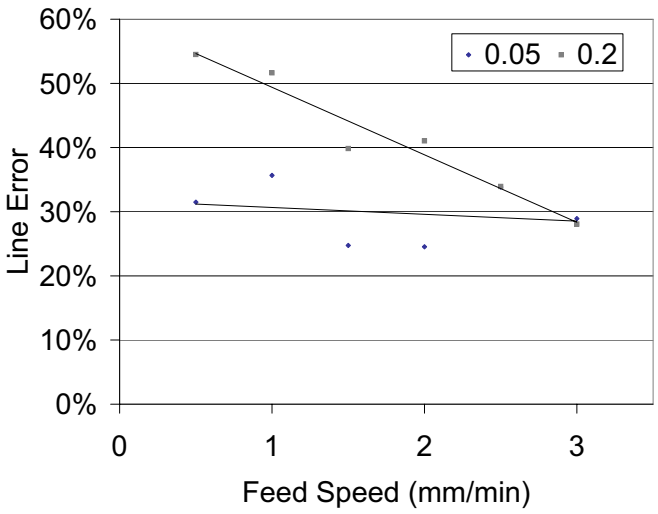

Figure 3.7: Straight line error verses feed speed and d.o.c. (µm)

In comparing these results with those previously obtained, there data does not follow a general trend. Figure 3.8 shows that the second stage outperformed the first for cuts made at a depth of 5µm while Figure 3.9 shows the opposite trend for cuts made at 20µm. This suggests that each stage was able to perform well as the accuracy was close the measurable limit with the equipment used.

3.2.2 Two-Dimensional Circular Trajectory Tests

Again patterning the tests conducted for the first stage, several circle following tests were performed. For these experiments the machine tool slot milled circles of various sizes, and then both the inner and outer edges of these circles were examined. The inner radii ranged from 10 - 50µm and the depth-of-cut was twenty microns.

Figure 3.10 shows a comparison of the error between the two edges. Similar to the trend observed in with the tests completed with the first stage machine, the errors moved in opposite directions. However in this case, the error of the outer edge increased by only a very small amount.

A more thorough comparison of the outer edge error for two stages is shown in Figure 3.11. The data is plotted in the log scale to better illustrate two important results. The first is that data points for the second stage are centered around the

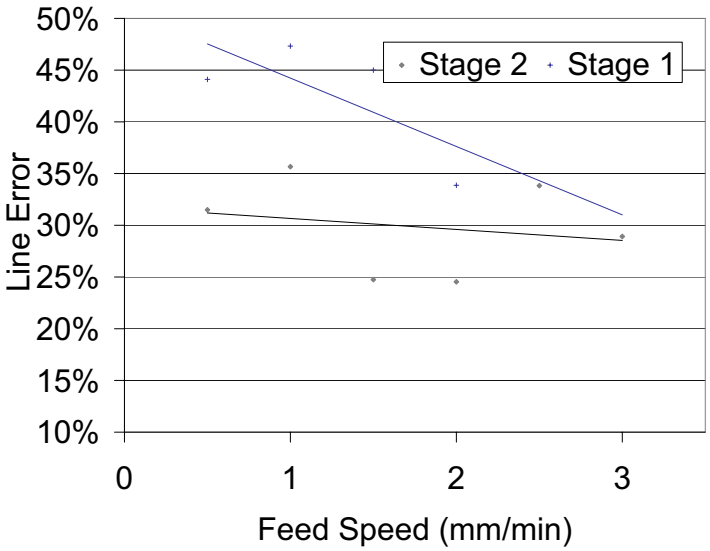

Figure 3.8: Line error for d.o.c of 0.05μm

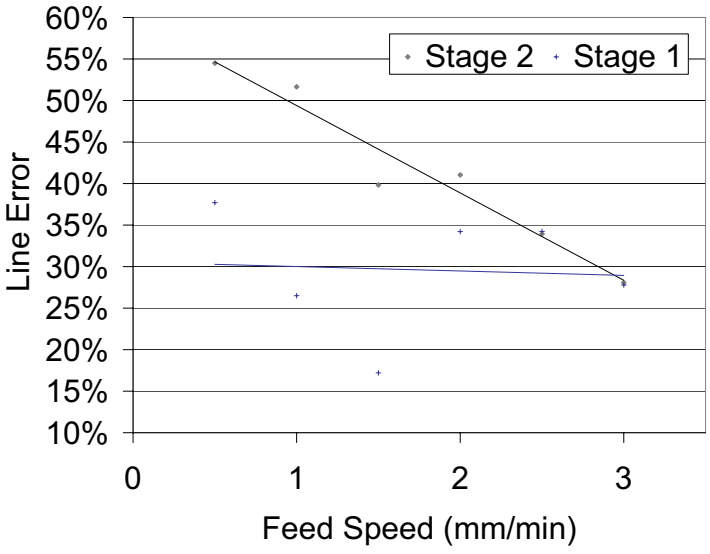

Figure 3.9: Line error for d.o.c of 0.2μm

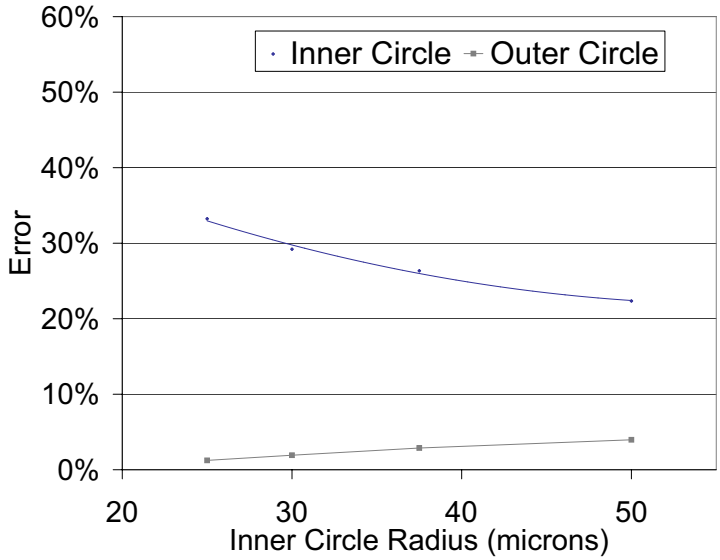

Figure 3.10: Errors for the inner and outer edges

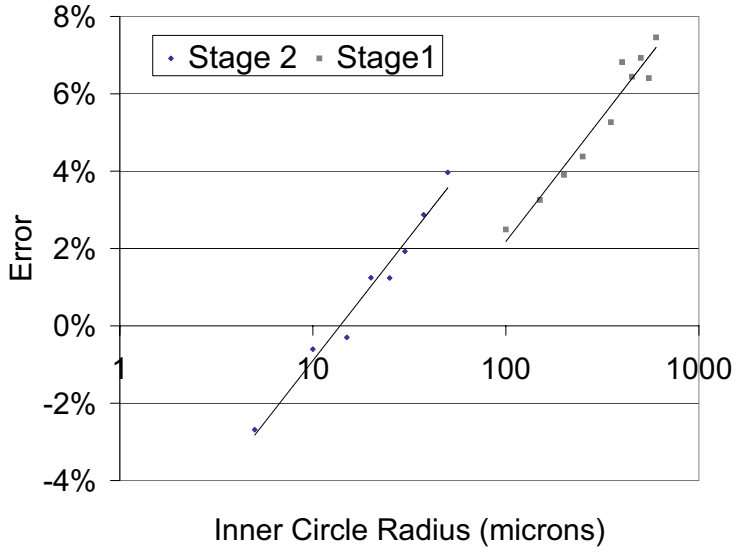

Figure 3.11: Standard deviation of the outer edges of circles for stages one and two verses the circle radius

x-axis, which indicates the circles have an overall lower error. The second is that the trend line for the second stage is shifted to the left, which shows that the achievable circle size is also reduced. In each of the two cases, the circles were machined in decreasing radius size until the inner portion was no longer measurable. (At that point, the inner circle appeared like a large burr and none of its dimensions could be measured by the inferometer as its surface geometry was very irregular). The smallest circle possible with the second stage had a ten micron radius, which is significantly less than the circles with inner radius 50μm machined in the first stage.

3.2.3 Three-Dimensional Feature Tests

Again a series of three-dimensional tests were performed upon the machine tool. The experiments conducted during this stage were broader than those performed during the first stage, which were limited to simple surface contours and submillimeter ($\geq$0.5mm) sized parts. This time the machine tool produced several actual micro-scale parts which included a hemisphere, bolt, and gear.

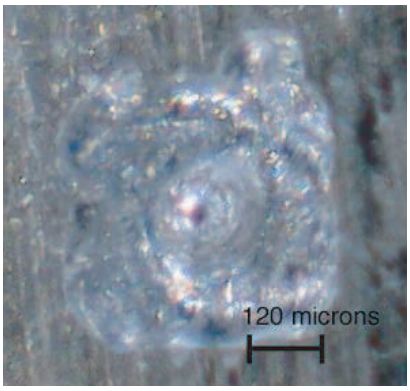

Figure 3.12: Machined micro-hemisphere

The first and simplest part made was a micro hemisphere. It had a radius of the of 120μm. The Z-direction step size used for machining the part was 15μm. A basic top view of the part is shown in Figure 3.12.

In seeking to produce a slightly more complicated part, a micro bolt was machined. This part is basically a quarter sphere connected to a half cylinder. Figure 3.13 shows the computer model which was used to generate the CNC code for the part next to

the actual micro bolt. The radius of the bolt head is 170μm and the shaft has a length of 340μm and radius of 70μm.

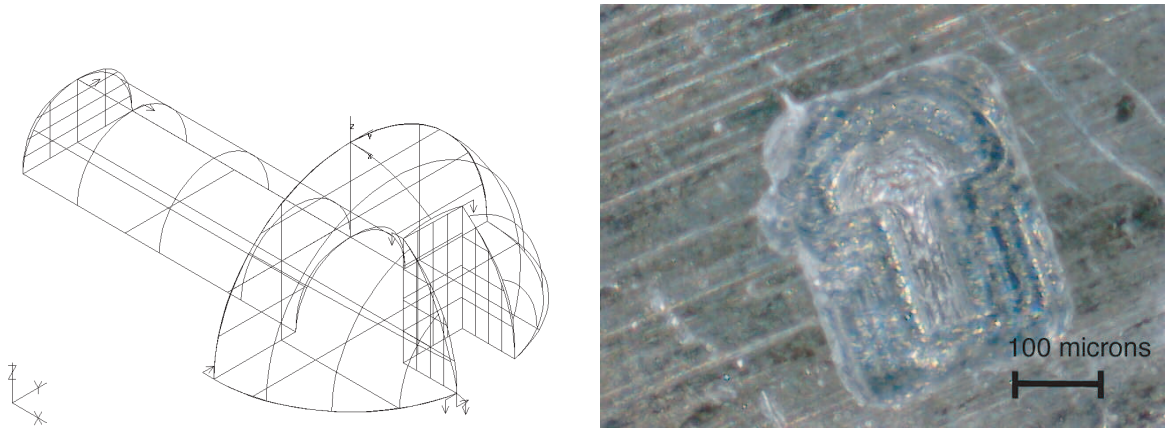

(a) (b)

Figure 3.13: Stages of micro bolt fabrication (a) computer generated wire-frame model (b) top view of the machined bolt

The micro gear was based upon the same computer model (see Figure 3.14a) used for milling gear shapes with the first stage. However the gears created with this setup, like the one shown in Figure 3.14b, were several times smaller than those previously made. As can be seen from Figure 3.15, the part was around 150μm in width, which is more than three times smaller than the parts achievable with the first stage.

The significance of these results is twofold. Firstly, the production of these parts demonstrates the machine tool's ability to generate fully three-dimensional micro-scale parts and features. In addition, these tests further illustrates the machine tool's ability to fully operate as a CNC milling machine.

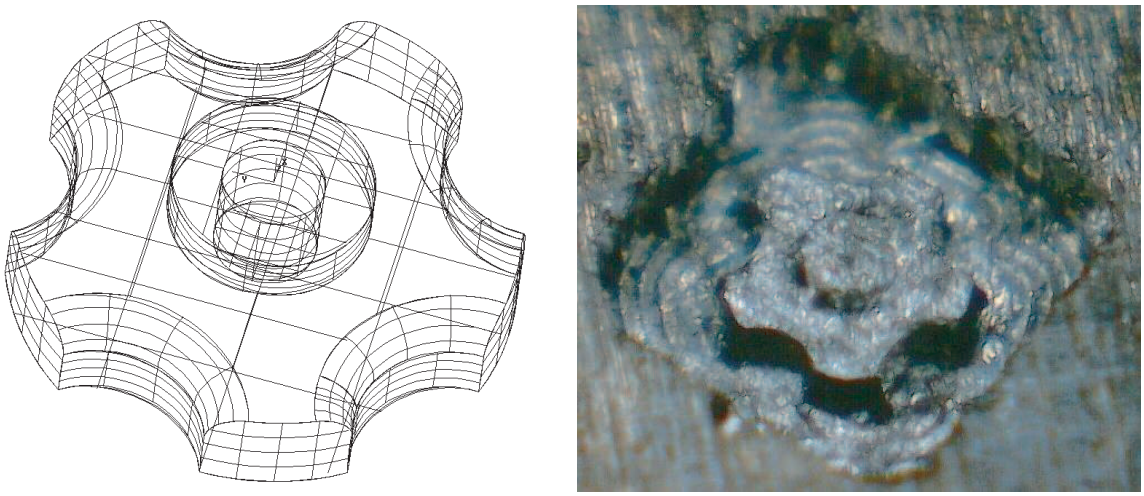

(a) (b)

Figure 3.14: The micro gear (a) computer generated wire-frame model (b) picture taken with the digital camera of the machined gear

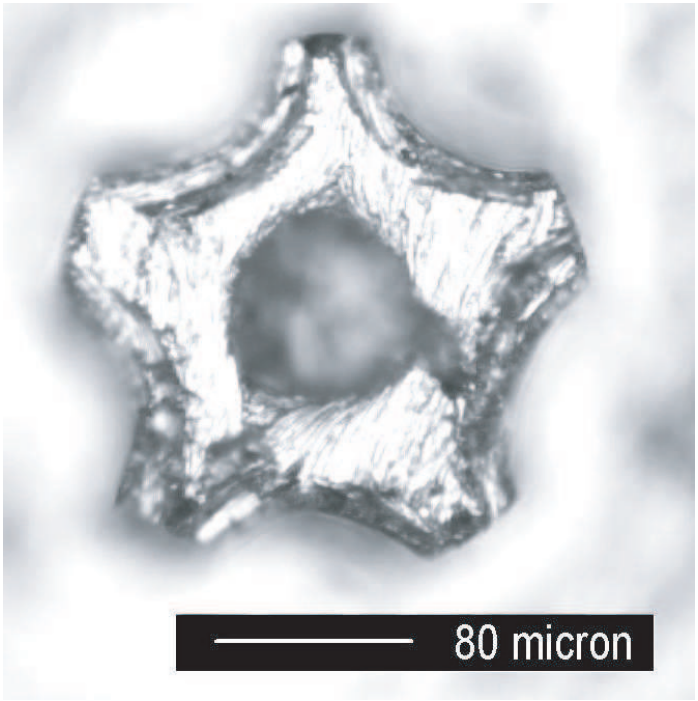

Figure 3.15: Microscope image of the top surface of the micro gear

Chapter 4

Theoretical Model

Theoretical models are important for gaining a better understand of the limits of miniaturized cutting. Following are the details of the force cutting model used herein.

4.1 Basic Force Model

An analytical model was developed to approximated the cutting forces on the micro end mill. The first approximations were based upon a two-dimensional orthogonal cutting model. Following are the steps taken to create the model. First, the machining power is calculated by the material removal rate multiplied by the specific cutting energy.

Material removal rate

$$\text{MRR} = a * d * v_f \tag{4.1}$$

And the specific cutting energy is taken as a function of undeformed chip thickness, given by [25]

$$\log u_c = -0.38 - 0.46 \log h_{ave} \tag{4.2}$$

which may be rewritten as

$$u_c = 10^{(-0.38 - 0.46 \log_{10}(h_{avg}))} \tag{4.3}$$

Here the average chip thickness is found using a simple two dimensional geometry model given below (see reference [25] for a full derivation).

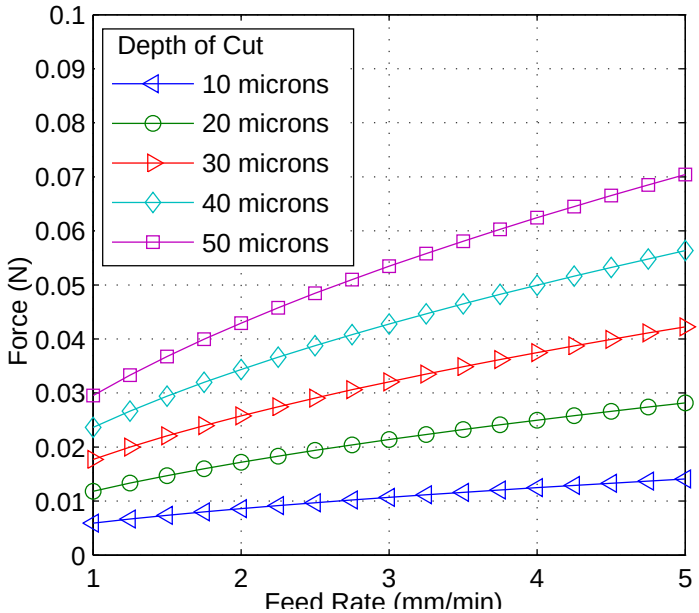

Figure 4.1: Theoretical cutting force curve for a 100µm tool shown with for series depth-of-cuts

$$h_{avg} = \frac{s_z \cos k(2(a_1 + a_2))}{D\left(\sin^{-1}(\frac{2a_2}{D}) + \sin^{-1}(\frac{2a_1}{D})\right)} \tag{4.4}$$

Coupling the above formulas results into a basic average power equation, $P_{avg} = u_c\text{MRR}$, makes it possible to compute an average force estimate by dividing the power by the rotational speed. Using a spindle speed of 60,000rpm and assuming a tool diameter of 100µm, the average cutting forces can be calculated and are graphed in Figure 4.1.

4.2 Maximum Cutting Conditions

Using the force model described in section 4.1, critical cutting conditions were determined in terms of depth-of-cut and feed speed. Using the experimental data from cases where the tool broke, it is possible to use determine a maximum allowable stress for these tools. Back solving the above equations using this stress will give an estimate of the allowable cutting conditions. Figure 4.2 shows a graph of these results. This model can then be compared to other experimental data to provide validation

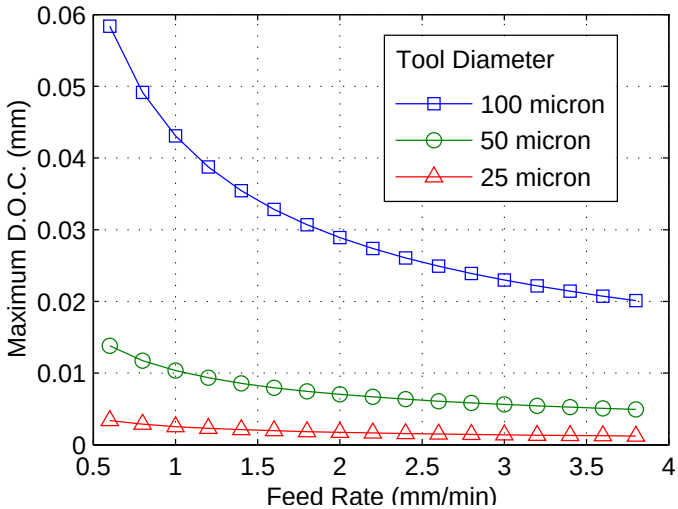

Figure 4.2: Maximum cutting conditions for a series tool diameters

for the model. A comparison for the case of a 100μm tool with a spindle speed of 60,000rmp is shown in Figure 4.3.

4.3 Force Measurement

The cutting forces were measured using a miniaturized dynamometer. Here the primary motivation behind measuring the cutting forces was to verify the cutting model previously developed. As noted earlier, the instrument used to measure the cutting forces was a Kistler milticomponent dynamometer. It was mounted between the lift stage of the positioning table and the work holder. For the actual force measurement, basic slot milling operations were performed. Three conditions were varied (feed speed, depth-of-cut and tool diameter) using three values for each condition. These values were used in combination with one another for a total of twenty-seven test cases, which are detailed in Table 4.1. The results are graphed in Figures 4.4 - 4.8. To remove the noise produced by the spindle, all the measurements were filtered with a low-pass filter and a band-reject filter that blocked the spindle's rotational frequency.

Initial attempts to collect cutting force data used conditions identical to those in

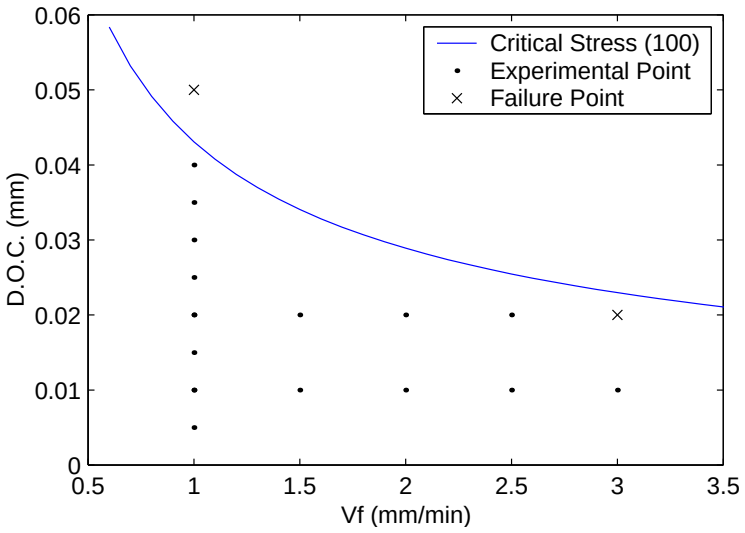

Figure 4.3: Experimental data plotted with a theoretical failure curve for a 100µm tool

the experimental sections. However these forces were found to be so small that it was not possible to reliably measure the output signal. Therefore, larger tools were used to allow for deeper cuts and higher feed rates so that the resulting force would be larger. As can be seen from graphs in Figure 4.4 - 4.8 there was still a significant variance in the force. To compensate for this, the force was averaged over the cutting region and the linear average is shown along with force in each of the graphs. The average also illustrates how the measured force typically decreases during the interval which is characteristic of piezoelectric force sensors. Therefore the cutting force was taken as the initial average value at the beginning of each cutting interval.

Even though there are several non-ideal factors influencing the cutting force measurements, they may still be used to for the original purpose. After an average cutting force was determined for each test, this number was then plotted on a theoretical force curve like the ones mentioned earlier. Figure 4.9 shows the comparison between the measured and theoretical cutting forces for these tests. In this graph, the outlined points indicate experimental data and the vertical distance from them to the theoretical curve represents the error. This comparison is not a perfect one as the model predicts cutting force while the graphs show the feed force. It was attempted to measure the cross feed force as well, however the results varied significantly. The plots

Table 4.1: Range of test variables used for measuring the cutting forces

Test	1	2	3	4	5	6	7	8	9
v_f (mm/min)	1	2	3	1	2	3	1	2	3
D.O.C. (mm)	0.02	0.02	0.02	0.03	0.03	0.03	0.04	0.04	0.04
Tool Dia. (μm)	300	300	300	300	300	300	300	300	300
Test	10	11	12	13	14	15	16	17	18
v_f (mm/min)	1	2	3	1	2	3	1	2	3
D.O.C. (mm)	0.02	0.02	0.02	0.03	0.03	0.03	0.04	0.04	0.04
Tool Dia. (μm)	500	500	500	500	500	500	500	500	500
Test	19	20	21	22	23	24	25	26	27
v_f (mm/min)	1	2	3	1	2	3	1	2	3
D.O.C. (mm)	0.02	0.02	0.02	0.03	0.03	0.03	0.04	0.04	0.04
Tool Dia. (μm)	800	800	800	800	800	800	800	800	800

of the recorded cross feed force are shown in Figures 4.10 - 4.14. Due to the erratic nature of this data, a reasonable measurement of the total cutting force could not be made. This necessitates resorting to the form of comparison made herein.

There is a noticeable discrepancy between the theoretical and actual measurements. The variance is adequately pronounced so that there are several readily visible error trends: the experimental force data is consistently lower than the experimental data, the disparity is also more pronounced for larger tool sizes, there was a significant amount of noise for cases where the average force was around or below 10mN. Yet these results do indicate that the force model may be practical as a first approximation for certain cases such as those with a smaller tool size. Additionally, significantly reducing the error of the calculated average cutting force beyond 20-30% seen in these cases may only be moderately useful. As seen in from many of these cases, the actual cutting force has an initial spike from fifty to one hundred percent of the initial average value. In spite of these drawbacks, the model allow for meaningful results for a certain range of cases and does give fairly accurate failure predictions for smaller sized tools.

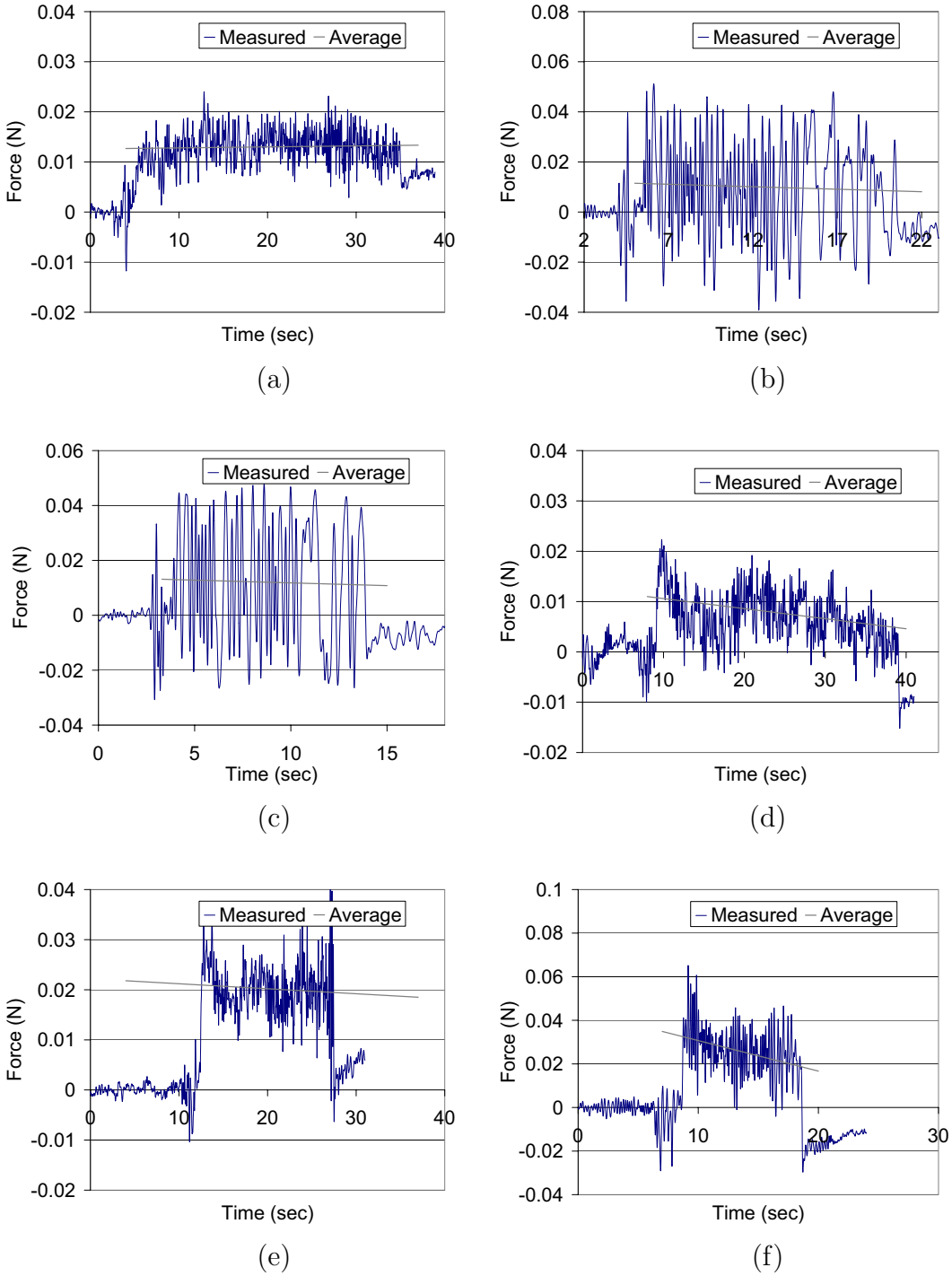

Figure 4.4: Measured feed forces: Test 1 (a) through Test 6 (f)

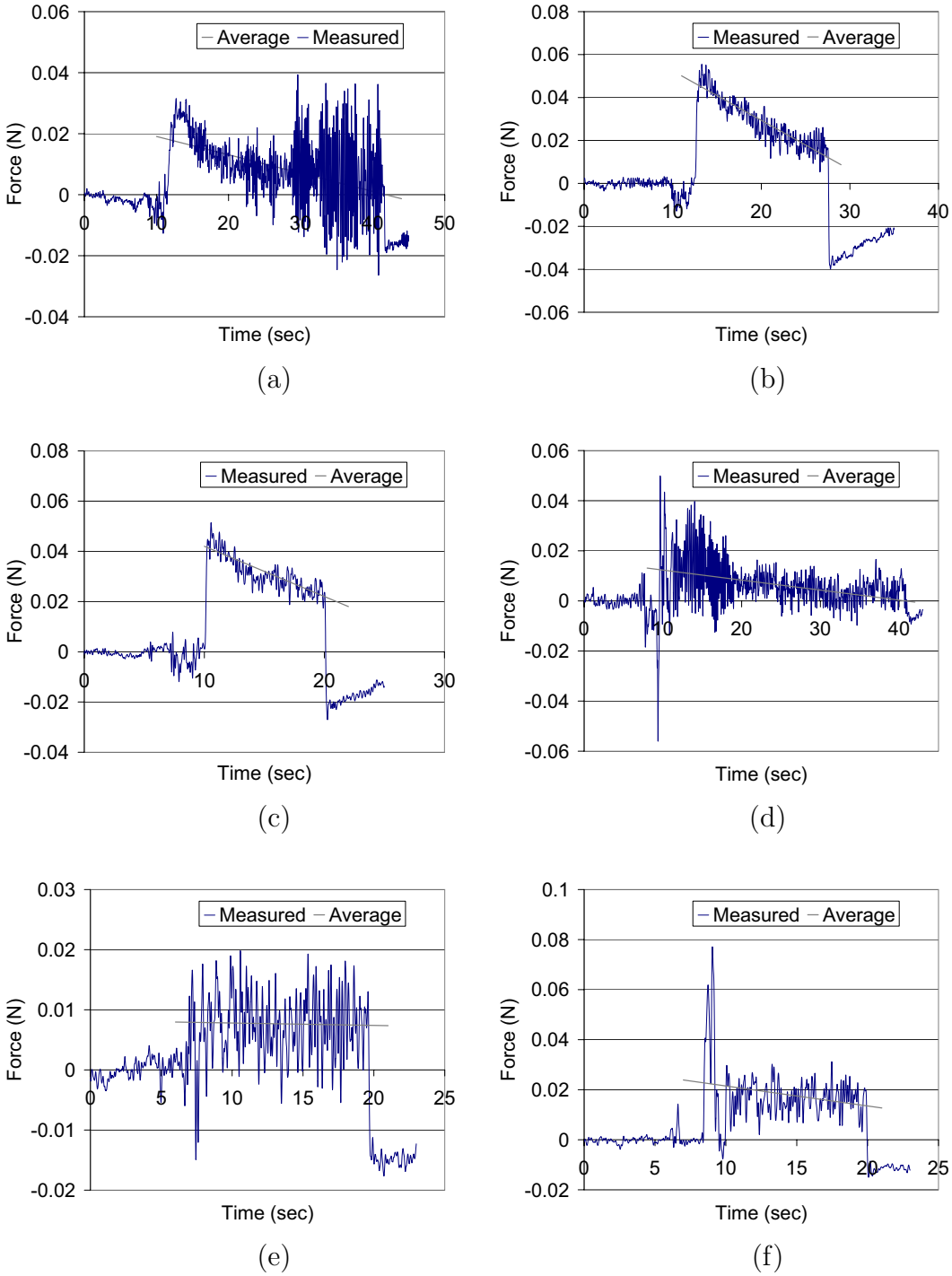

Figure 4.5: Measured feed forces: Test 7 (a) through Test 12 (f)

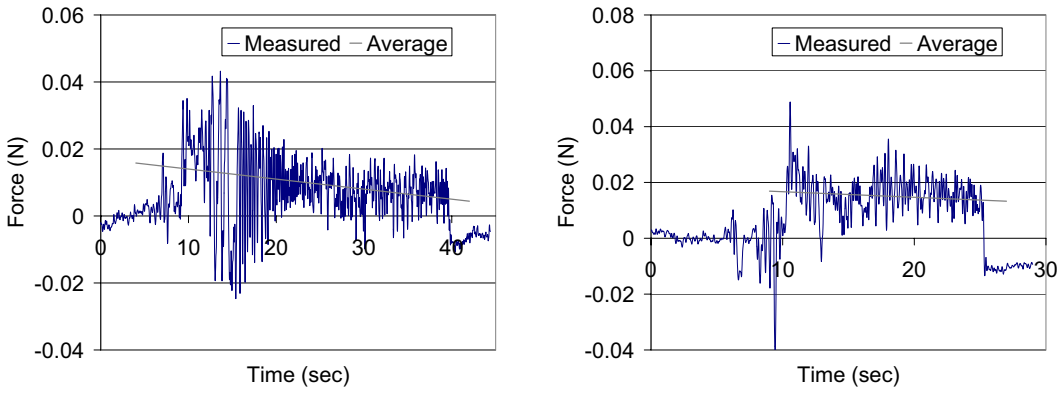

(a)

(b)

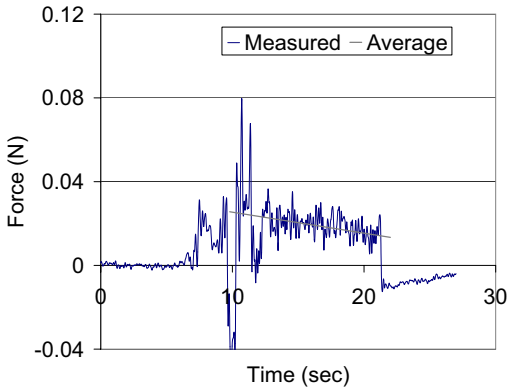

(c)

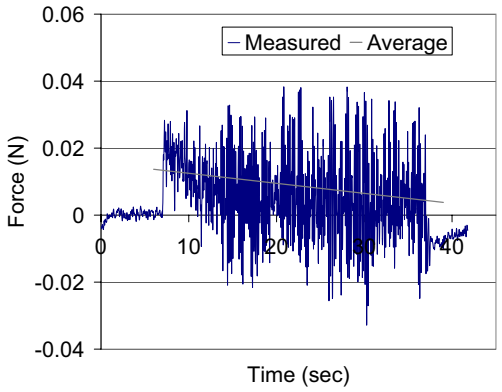

(d)

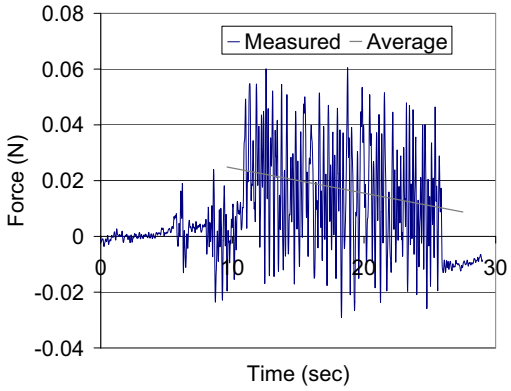

(e)

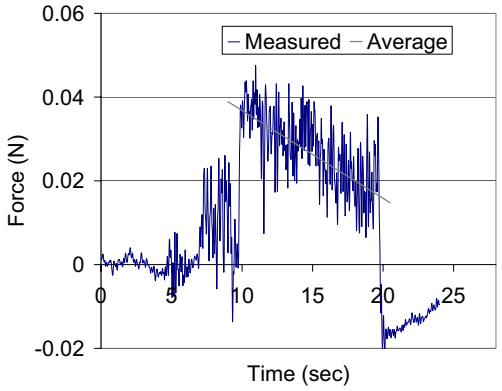

(f)

Figure 4.6: Measured feed forces: Test 13 (a) through Test 18 (f)

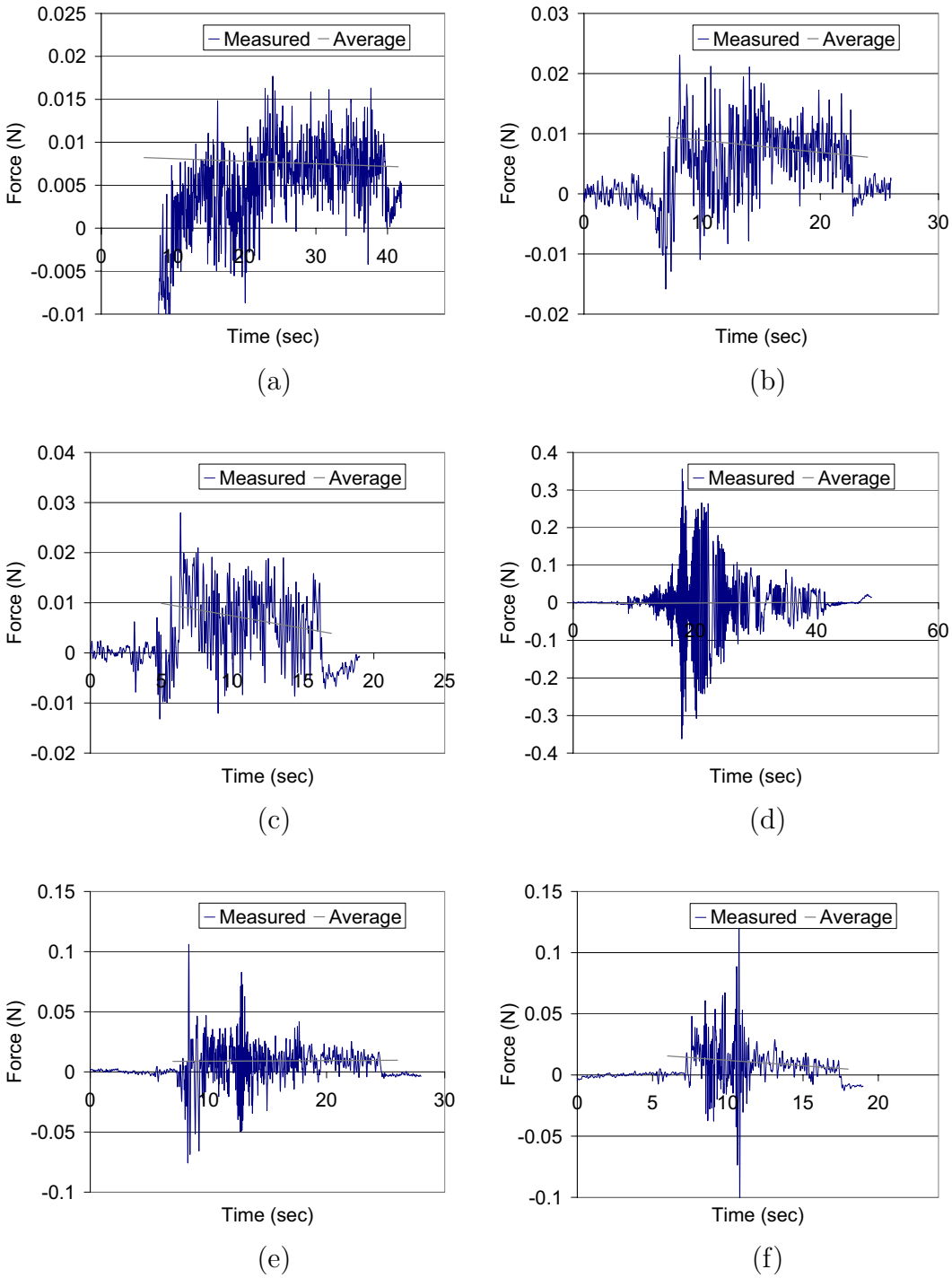

Figure 4.7: Measured feed forces: Test 19 (a) through Test 24 (f)

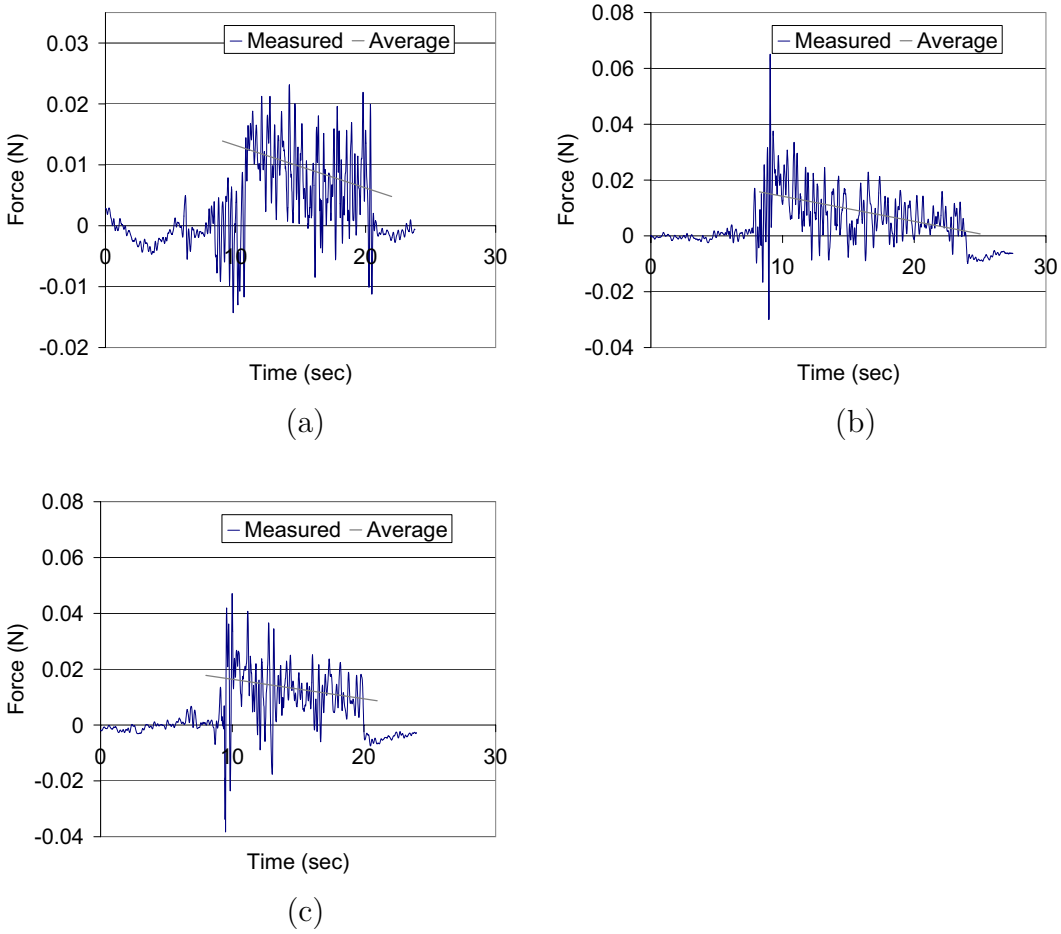

Figure 4.8: Measured feed forces: Test 25 (a) through Test 27 (c)

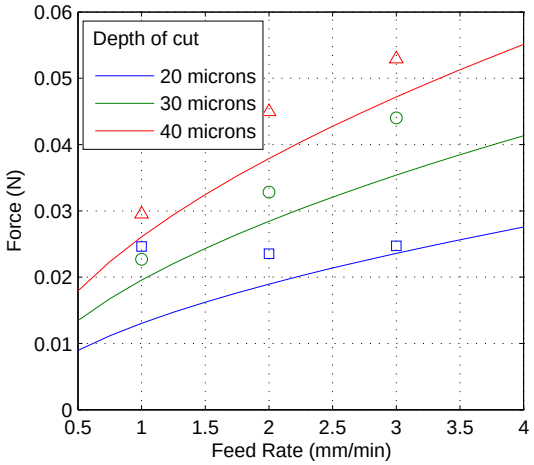

(a)

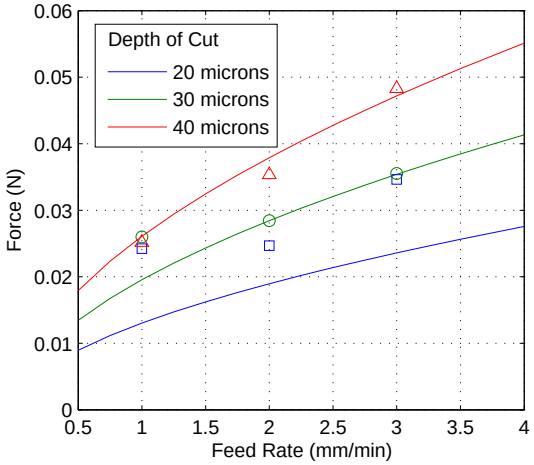

(b)

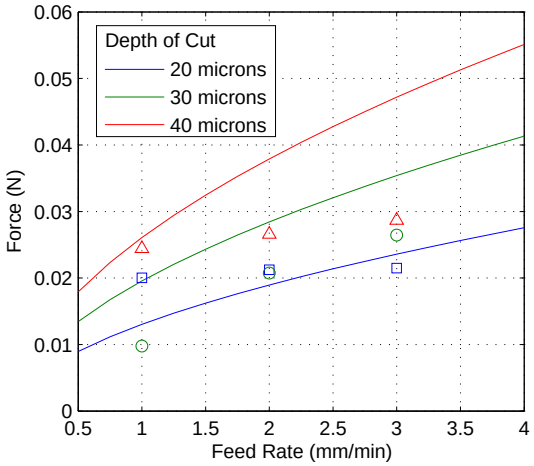

(c)

Figure 4.9: The theoretical cutting forces compared to the measured average for (a) 300µm tools, (b) 500µm tools and (c) 800µm tools

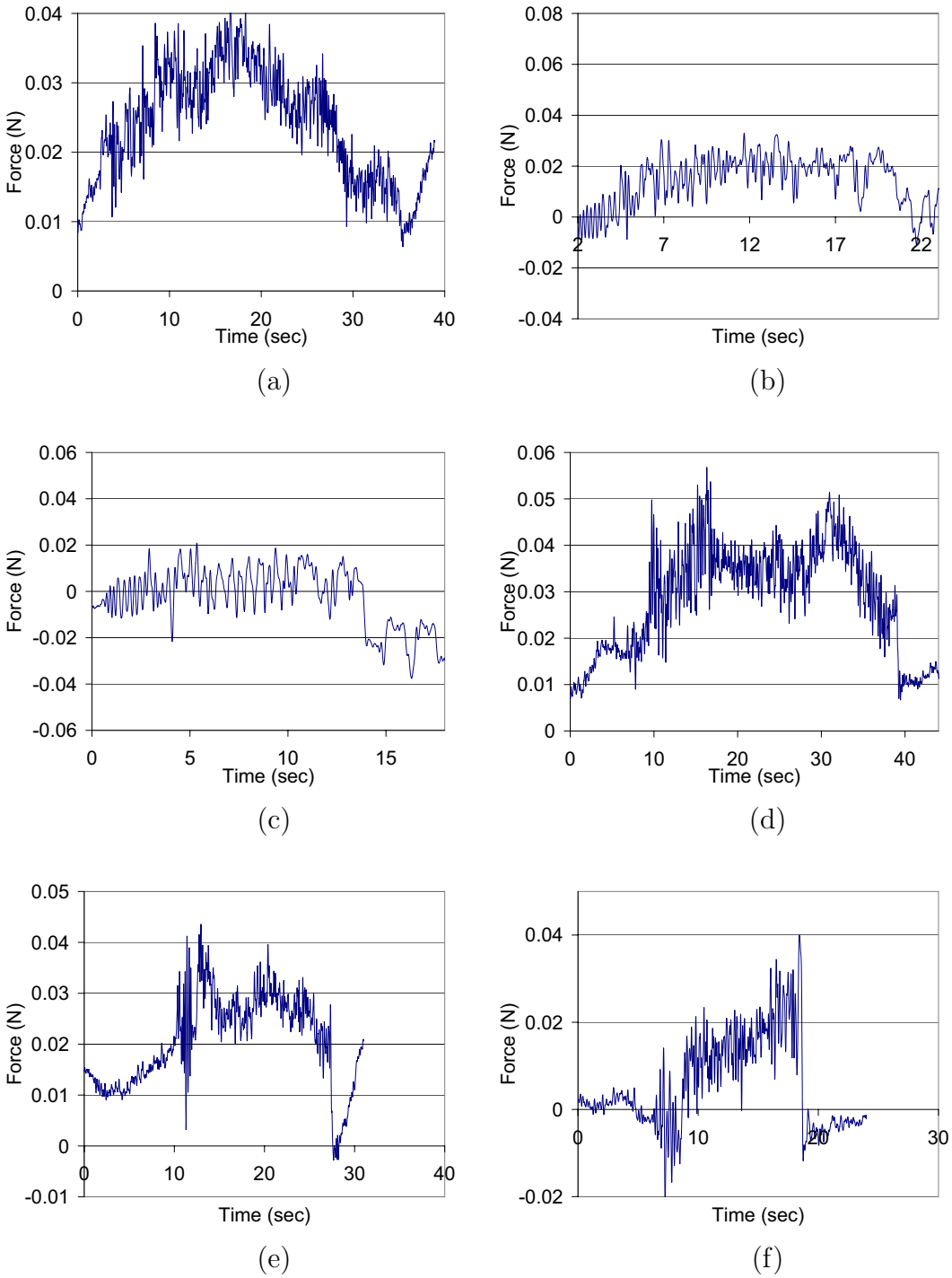

Figure 4.10: Measured cross feed force: Test 1 (a) through Test 6 (f)

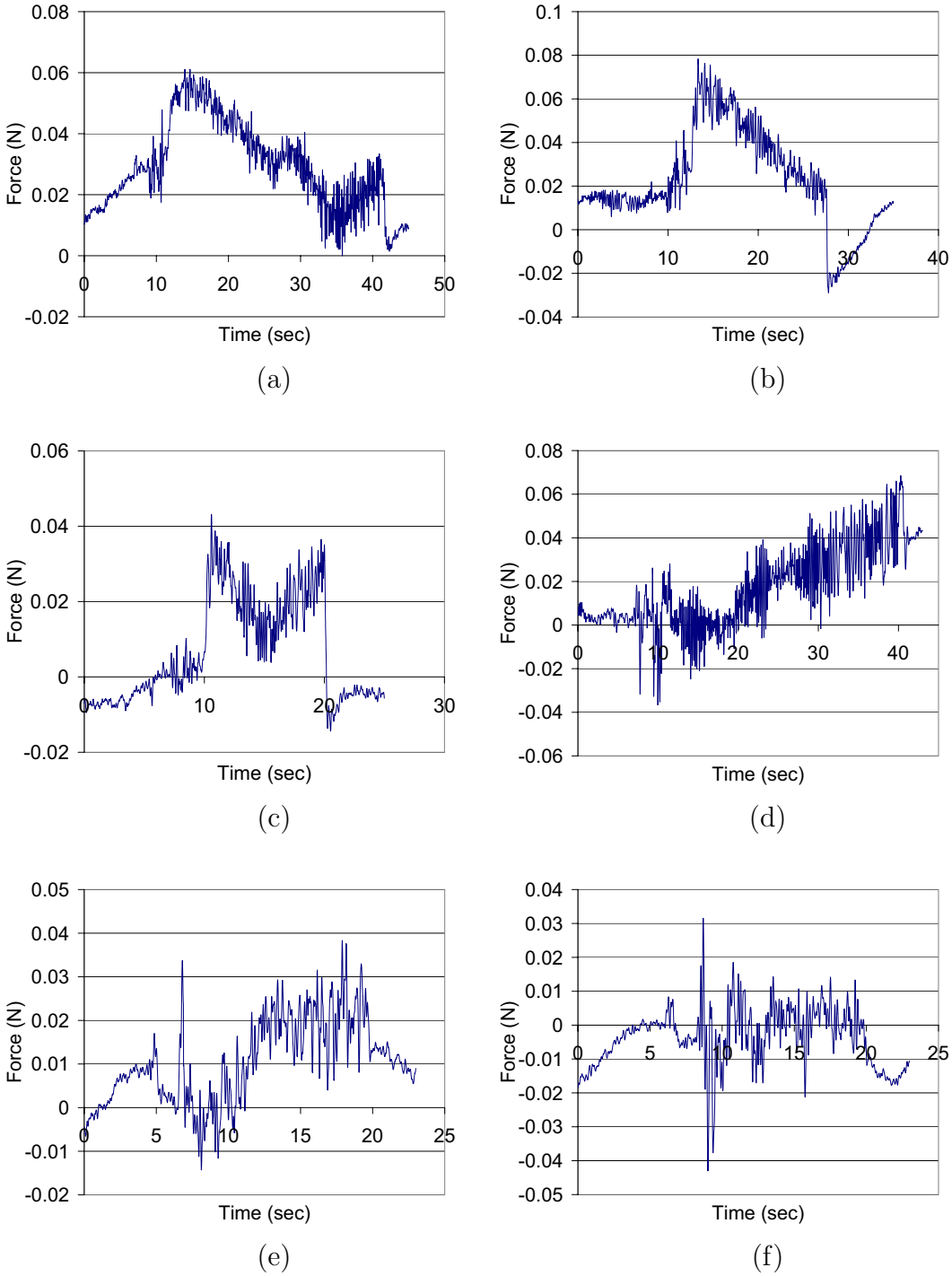

Figure 4.11: Measured cross feed force: Test 7 (a) through Test 12 (f)

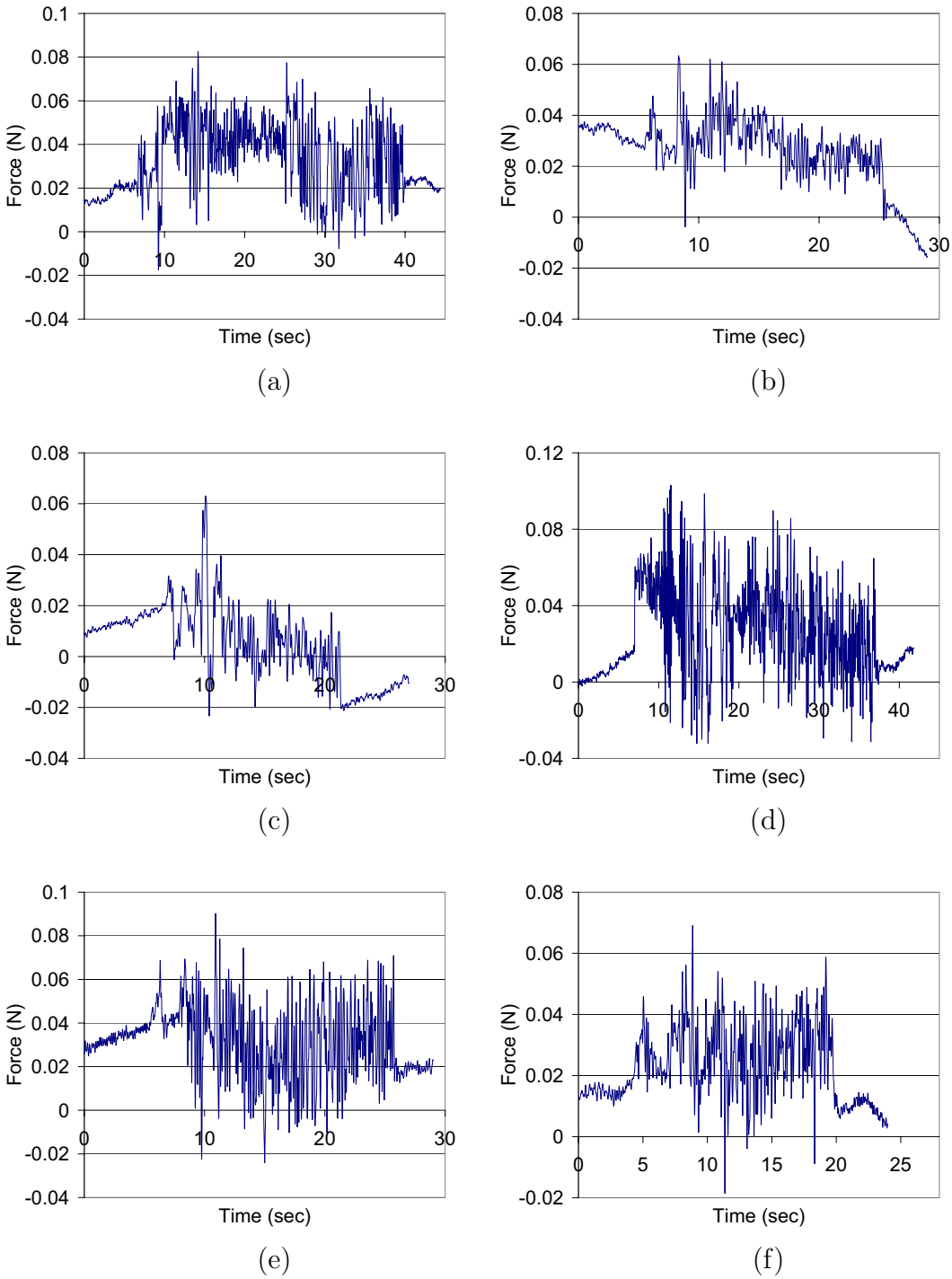

Figure 4.12: Measured cross feed force: Test 13 (a) through Test 18 (f)

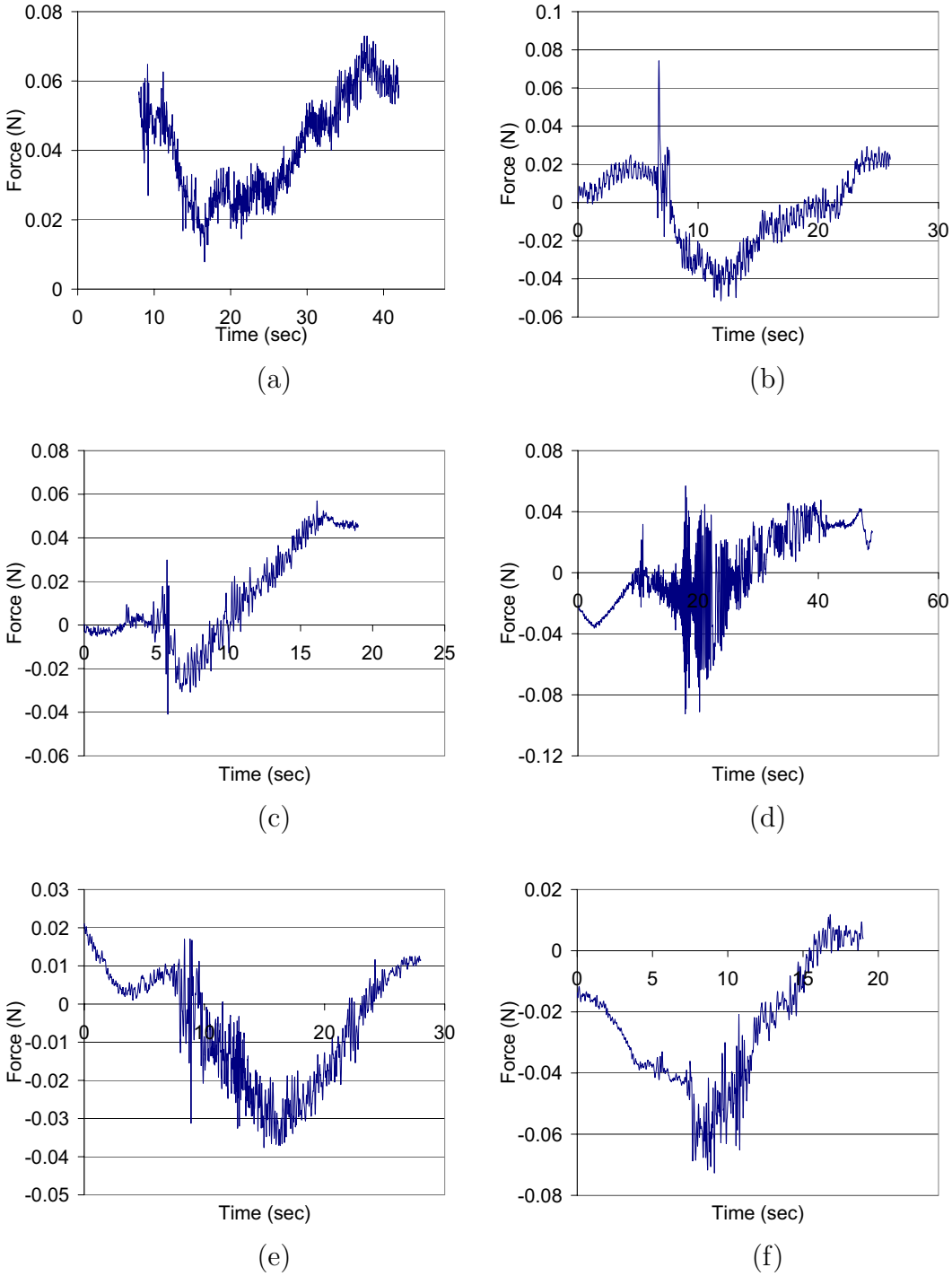

Figure 4.13: Measured cross feed force: Test 19 (a) through Test 24 (f)

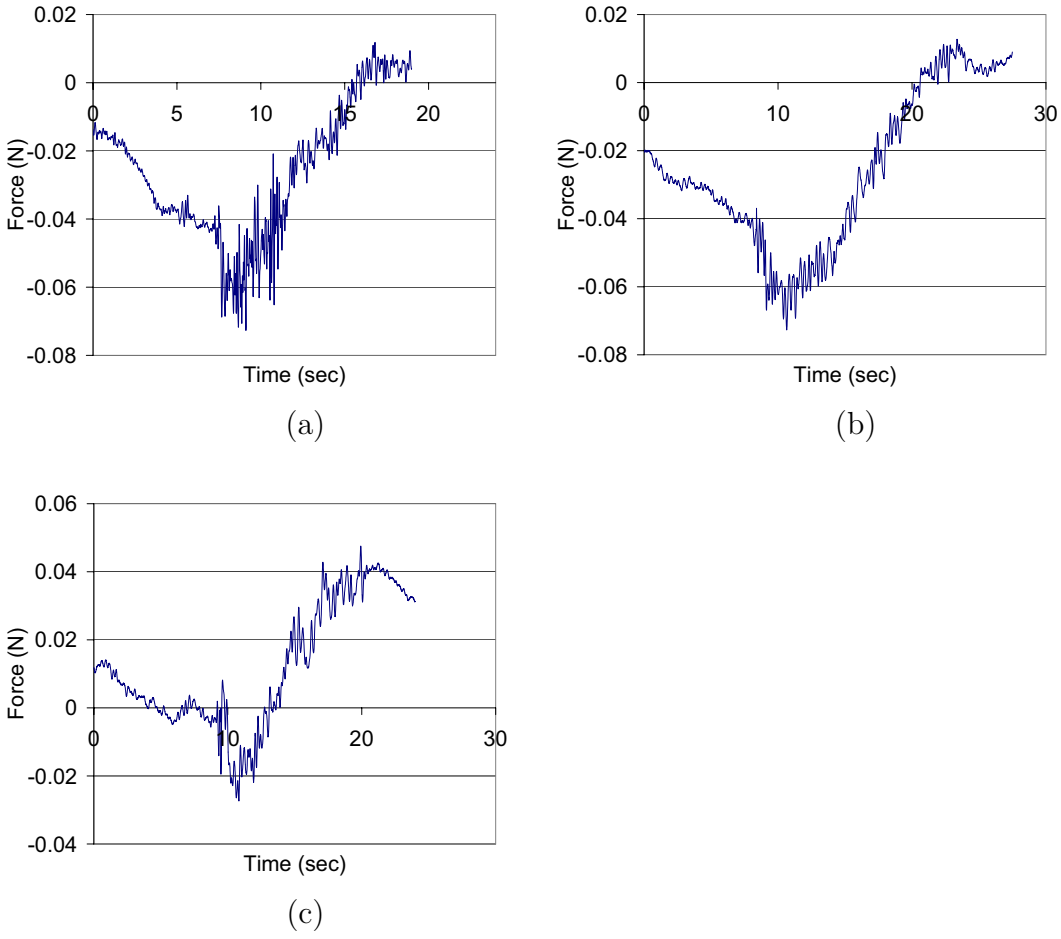

Figure 4.14: Measured cross feed force: Test 25 (a) through Test 27 (f)

Conclusion

This paper has addressed the development and testing of a miniaturized machine tool. After briefly looking at the motivation behind miniaturization, it summarized several pieces of work that have already been completed and proposed some basic contributions that may be performed in this field. These being, the fabrication of 3-D free from features on the micro scale, the implementation of meaningful benchmarks for a micro milling machine, and the formation of a basic cutting force model.

The design and configuration of a microscale vertical machining center of overall dimension less than 0.1m^3 has been presented and the component specifications discussed. To quantify the performance capability of the microscale machine tool as a system, a series of evaluation tests were implemented based on 1-D linear trajectory, 2-D circular trajectory, 2-D arch trajectory, and 3-D part tests over a range of feed speed and depth of cut conditions. Test results suggest that micro level form accuracy and sub-micro level finish are generally achievable for parts with moderate curvature and gradient in the geometry under selected machining parameters and conditions.

Finally the paper presented a basic force model that would be applicable for the machining domain of the miniaturized machine tool. This model may be used as a practical guide in determining the limiting cutting conditions.

Machining parts and features on the micro scale is continuing to be developed and there remain many areas to be explored. Drawing specifically upon the work completed herein, there are likewise several possibilities for further exploration. Following are specific comments on some such potential areas.

Fully exploring the observed errors to identify their causes would also be a possible area for follow up. An understanding such as this could be used to develop methods for then reducing these errors. In particular, establishing the cause for the errors seen in the circle following tests involving small radii.

An additional area that may be more fully mapped out is measuring the cutting forces for the smaller sized tools. This could serve to better validate the cutting force model used herein and serve as a guide for refining this model. In addition, measurements of these small scale forces could be used to better investigate how specific cutting energies change for chips cut in the nanoscale.

As development in miniaturized machine tools moves forward, it greatly increases the potential for a fully miniaturized factory. Another important step towards this end would be to develop integration techniques to link these machines together. This could include miniaturizing automatic mechanisms for loading and unloading parts, aligning workpieces and workholders, and orienting workpieces. Such technology could very easily increase the functionality of a miniaturized machine tools.

Appendix A

Frame Design

The following section is quoted directly from reference [22] and is based upon work completed by H. W. Park. This work examines the machine size effect on static stiffness using an example case of a simplified column-and-knee type vertical machine tool shown in Figure A.1.

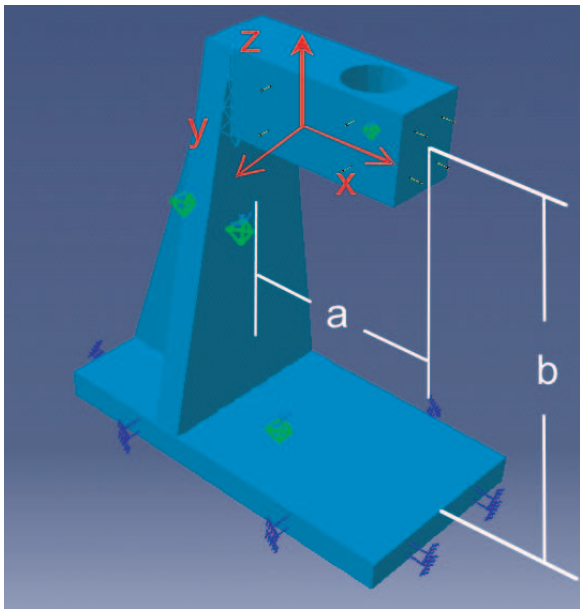

Figure A.1: Finite element model of a vertical machine tool

"In parallel to this argument on the size effect on accuracy classification is the structural size effect on the rigidity of the machine tool. In the context of dynamic rigidity and stability, the parameters of great importance are generally the damping

characteristics, effective mass, and static stiffness. As a 2^{nd}-order linear dynamical system of mass-spring-damper is considered to represent the dynamic behavior of a machine tool for rough approximation, the maximum amplitude magnification ratio at the natural frequency can be given by:

$$r_{\omega=\omega_{dn}} = \frac{A_{\omega=\omega_{dn}}}{F_{\omega=\omega_{dn}}} = \frac{\sqrt{m_{eff}/k_{static}}}{c} \tag{A.1}$$

where $A_{\omega=\omega_{dn}}$ is the magnitude response at the natural frequency, $F_{\omega=\omega_{dn}}$ the forcing amplitude at the natural frequency, m_{eff} the mass, k_{static} the static stiffness, and c the damping ratio. Therefore the size, and the overall mass of the machine tool m_{eff}, shows a strong effect on the dynamic rigidity of the machine to the square root power similar to what was argued in Reshetov and Protman [26]. The reduction of the machine tool size will increase the natural frequency, offering a wide range of machine tool operation frequencies without chatter instability. This occurs since the machining operation dynamics will be pushed toward the left side of a stability lobe diagram...

"In this study, finite element analysis was performed in order to quantitatively assess the performance advantages of the miniaturized machine tool center. Finite element analysis (CATIA-based) of the resulting static stiffness, as shown in Figure A.2a, for configurations of a fixed a/b=0.5 and with a fixed bottom surface of the supporting column (as it has less effect on the machining accuracy and precision than the spindle overhang and the column height) but with different overall machine sizes "a's" indicates that the stiffness in all vertical, lateral, and forward directions improve significantly as the machine size decreases. The static stiffness improvement by machine miniaturization will lower the low-frequency deflection and part form errors, and it also further feeds into the enhancement of dynamic rigidity and the achievable precision.

"As shown in Figure A.2b, the size reduction of a machine tool decreases its thermal expansion in response to the ambient temperature variation. The high and relatively constant values of thermal stiffness in the machine lateral direction stems from the basic symmetry of the structure. However, the increasing trend of the vertical and forward thermal rigidities with respect to smaller machine dimension suggests that the miniaturization of the machine can contribute to a higher resistance

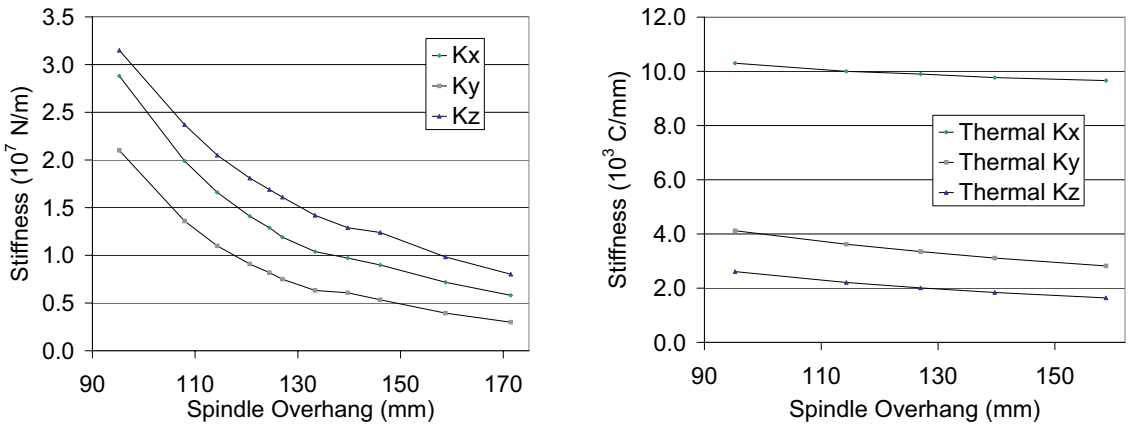

(a) (b)

Figure A.2: Theoretical frame models (a) static stiffness and (b) thermal stiffness as functions of the spindle overhang length

to temperature variation. This benefit is a result of the fact that less structural volume is involved in thermal expansion in the case of smaller machine tools. The quantitative understanding of the effects of machine tool miniaturization can provide a guideline for the evaluation, design, and optimization of the miniaturized machine structure and control mechanism."

Appendix B

Frame Schematics

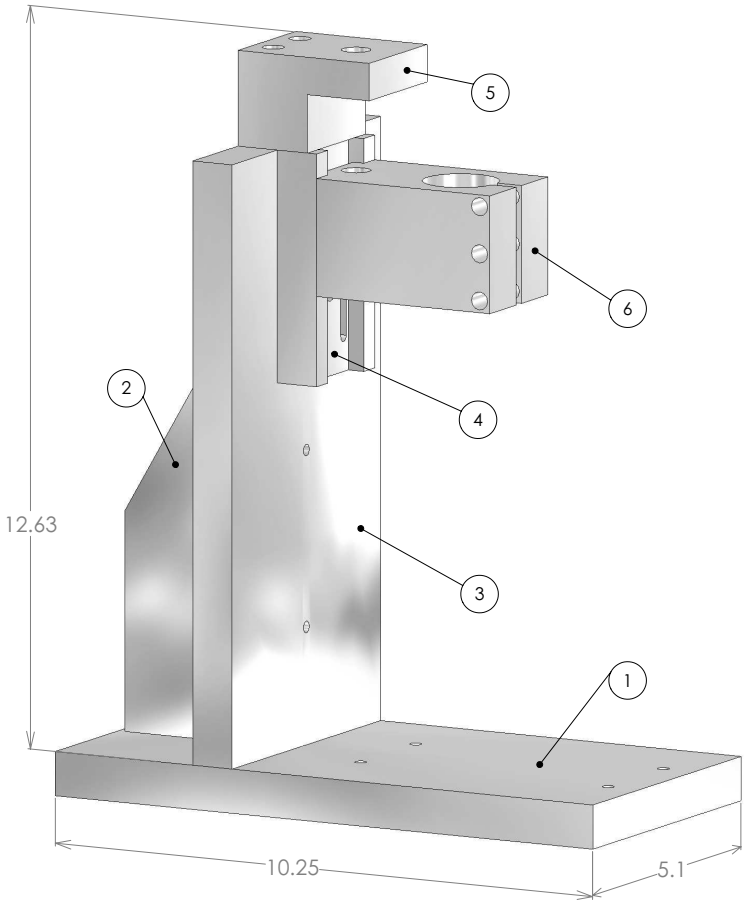

Computer generated model of the machine frame (all dimensions are in inches).

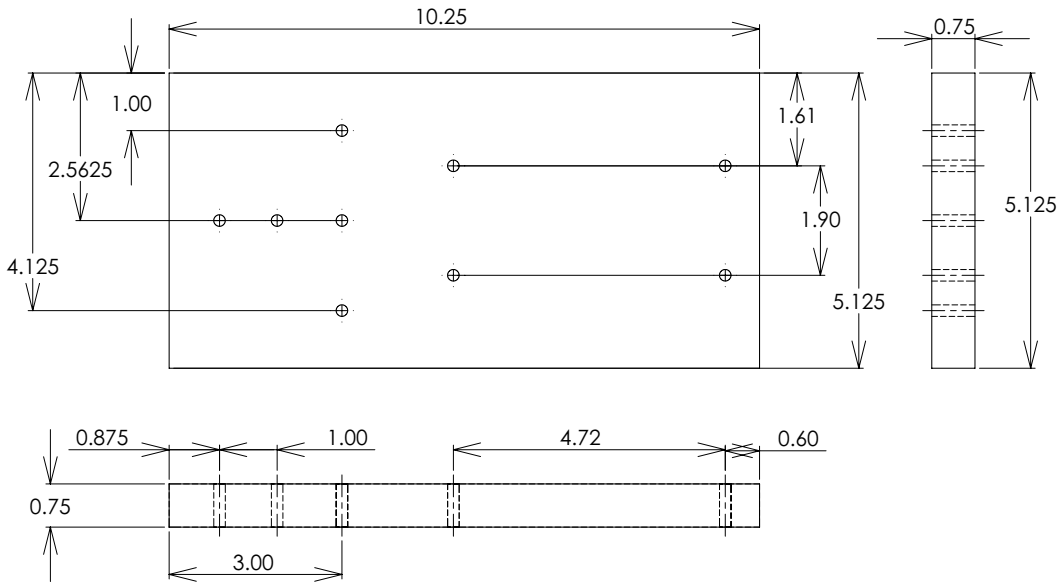

1. Base Plate

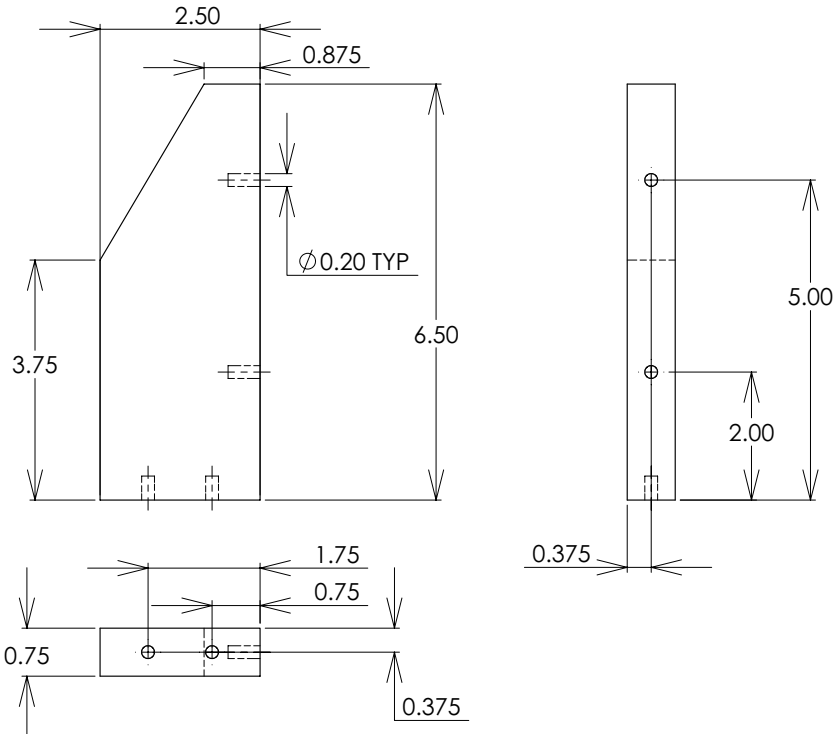

2. Back Support

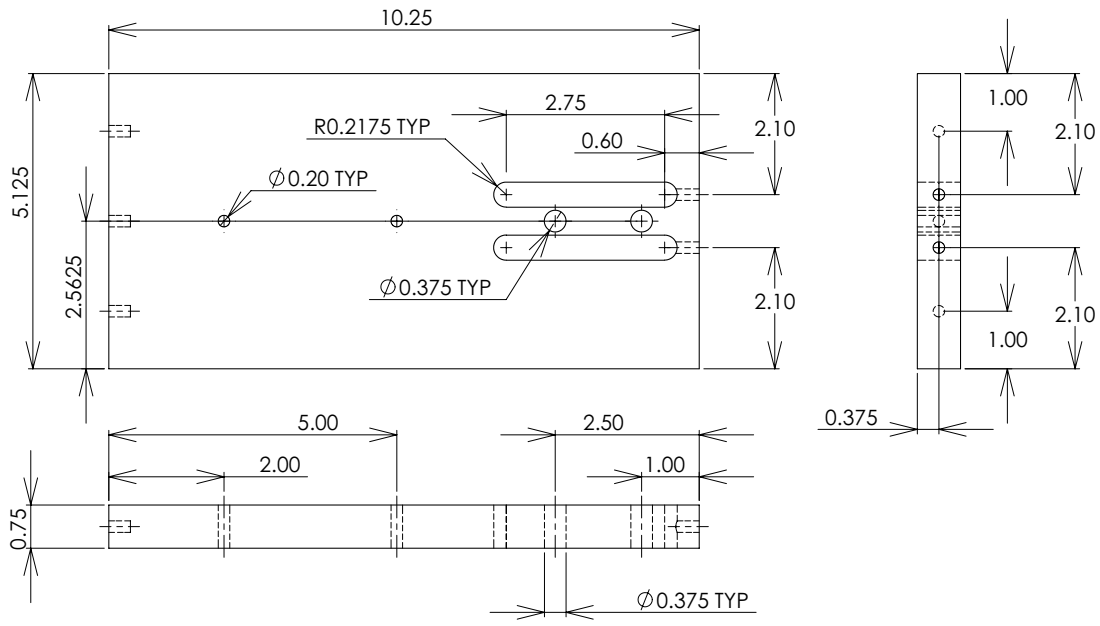

3. Frame Column

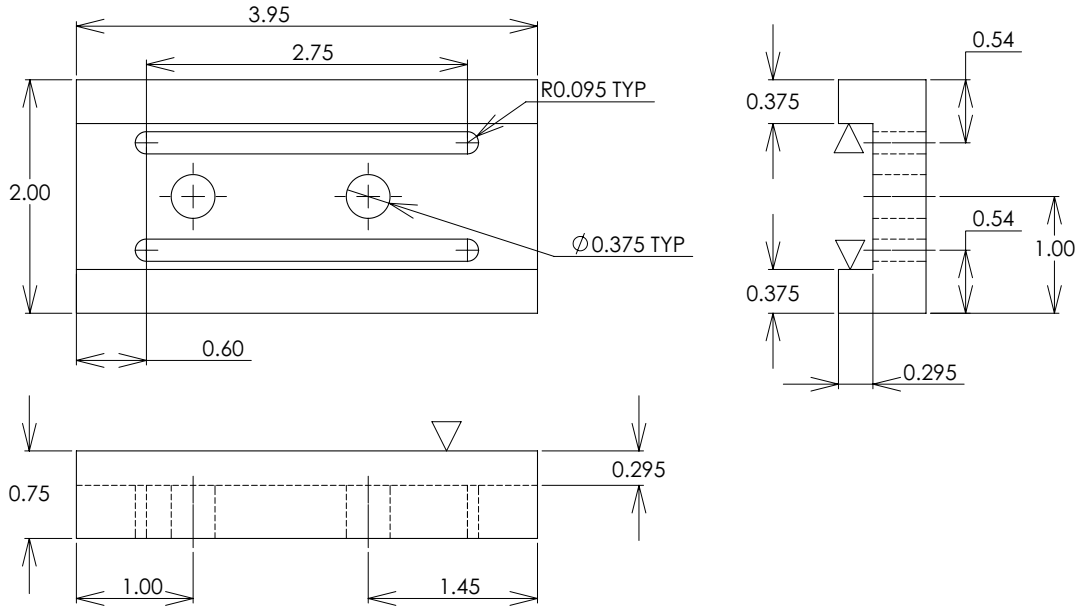

4. Back Mount

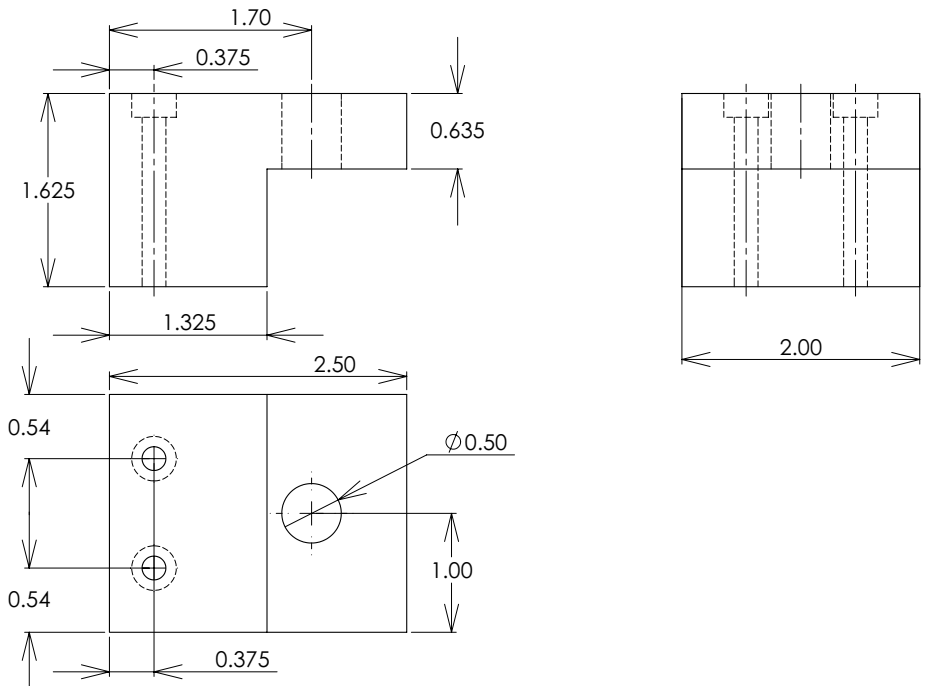

5. Top Holder

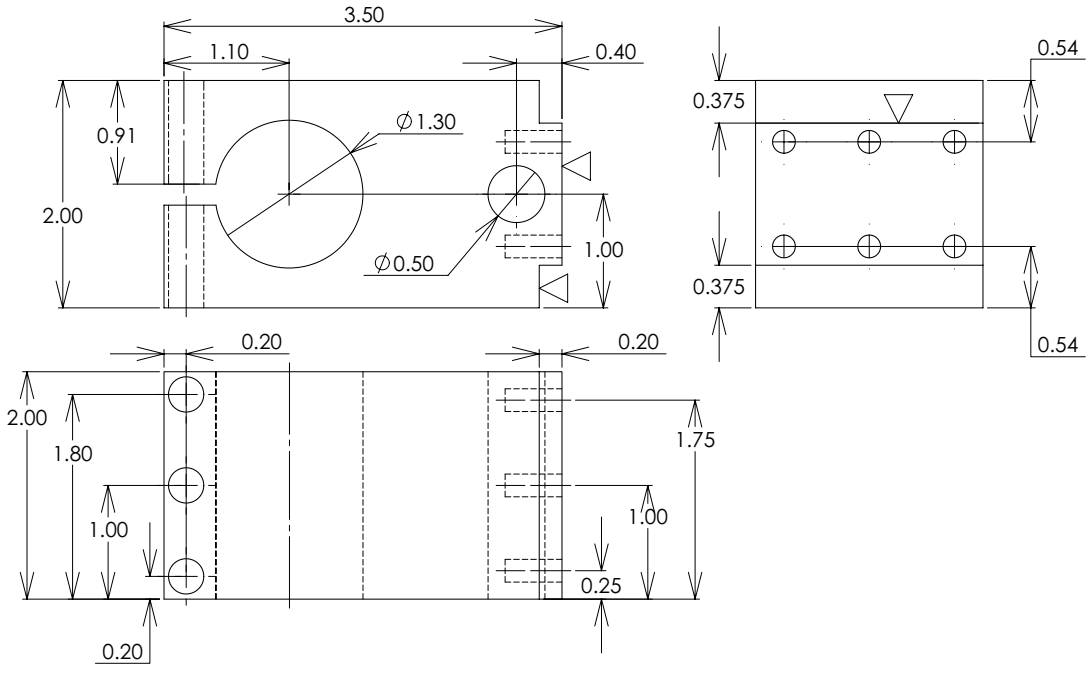

6. Spindle Arm

References

[1] CORBETT, J., MCKEOWN, P. A., PEGGS, G. N., and WHATMORE, R., "Nanotechnology: International Developments and Emerging Products," *Keynote Paper*, *Annals of CIRP*, vol. 49, 2002.

[2] MADOU, M., *Fundamentals of Microfabrication: the science of miniaturization*. CRC Press LLC, 2 ed., 2002.

[3] VASILE, M., FRIEDRICH, C., KIKKERI, B., and MCELHANNON, R., "Micrometer-scale machining: tool fabrication and initial results," *Precision Engineering*, vol. 19, pp. 180–186, 1996.

[4] SCHALLER, T., BOHN, L., MAYER, J., and SCHUBERT, K., "Microstructure grooves with a width of less than 50mm cut with ground hard metal micro end mills," *Precision Engineering*, vol. 23, pp. 229–235, 1999.

[5] TANSEL, I., RODRIGUEZ, O., TRUJILLO, M., PAZ, E., and LI, W., "Wear Induced Stress (WIS) and Tool Breakage in Micro-End-Milling," *Intelligent Engineering Systems Through Artificial Neural Networks*, vol. 5, pp. 867–872, 1995.

[6] FANG, F. Z.,WU, H., LIU, X. D., LIU, Y. C., and NG, S. T., "Tool Geometry Study in Micromachining," *Journal of Micromechanics and Microengineering*, vol. 13, pp. 726–731, 2003.

[7] OKAZAKI, Y., MORI, T., and MORITA, N., "Desk-top NC milling machine with 200 krpm spindle," *Proc. ASPE Annual Meeting*, pp. 192–195, 2001.

[8] LU, Z. and YONEYAMA, T., "Micro cutting in the micro lathe turning system," *International Journal of Machine Tools & Manufacture*, vol. 39, pp. 1171–1183, 1999.

[9] Vogler, M. P., Liu, X., Kapoor, S., DeVor, R., and Ehmann, K., "Development of Meso-Scale Machine Tool (mMT) Systems," *Trans of North American Manufacturing Research Institution*, pp. 653–661, 2002.

[10] Friedrich, C. R., Coane, P. J., and Vasile, M., "Micromilling development and applications for microfabrication," *Microelectronic Engineering*, vol. 35, pp. 367–372, 1997.

[11] Kussul, E., Baidyk, T., Ruiz-Huerta, L., Caballero-Ruiz, A., Velasco, G., and Kasatkina, L., "Development of micromachine tool prototypes for microfactories," *Journal of Micromechanics and Microengineering*, vol. 12, pp. 795–812, 2002.

[12] Lin, W., Ohmori, H., Uehara, Y., Asami, M., and Ohmori, M., "Development and Characteristic on the Desk-top 4-Axes Machine "TRIDER-X" for Micro-fabrication," *Proceedings of 4th International Workshop on Microfactories (IWMF2004) Shanghai, China*, pp. 74–79, October 15-17, 2004.

[13] Bao, W. and Tansel, I., "Modeling micro-end-milling operations. Part I: analytical cutting force model," *Internalional Journal of Machine Tools & Manufacture*, vol. 40, pp. 2155–2173, 2000.

[14] Mishima, N., "A Study on Optimization of Miniature Machine Tool Design," *Proceedings of 4th International Workshop on Microfactories (IWMF2004) Shanghai, China*, pp. 56–61, October 15-17, 2004.

[15] Wang, W., Kweon, S.-H., and Yang, S.-H., "Surface Roughness Study Based on Micro-End-Milling with a Miniaturized Machine Tool," *Proceedings of 4th International Workshop on Microfactories (IWMF2004) Shanghai, China*, pp. 104–109, October 15-17, 2004.

[16] Masuzawa, T., "Micromachining by Machine Tools," *Handbook of Sensors and Actuators*, vol. 6, pp. 63–82, 1998.

[17] Physik Instrumente (PI) GmbH & Co., "PZT Flexure NanoPositioners and Scanners ," *Physik Instrumente Nanopositioners Catalogue*, 2004.

[18] Aerotech Inc., "Linear Stages and Positioners," *Aerotech Inc. Product Catalogue*, 2004.

[19] ASM, *Metal Handbooks - Properties and Selection: Irons, Steels, and High-Performance Alloys*, vol. 1. ASM International, 10 ed., 1990.

[20] ASM, *Metal Handbooks - Properties and Selection: Nonferrous Alloys and Special-Purpose Materials*, vol. 2. ASM International, 10 ed., 1990.

[21] Davis, J. and Davis & Associates, eds., *ASM Specialty Handbook - Carbon and Alloy Steels*. ASM International, 1996.

[22] Cox, D., Liang, S., Newby, G., and Park, H. W., "Performance Evaluation of a Miniaturized Machining Center for Precision Manufacturing," *ASME International Mechanical Engineering Congress & Exposition, Anaheim, California*, November 2004.

[23] Newport Inc., "Workstations and Isolations Platforms," *Newport Product Catalogue*, 2004.

[24] Kistler Instrumente AG, "Cutting Force Measurment," *Kistler Product Catalogue*, 2004.

[25] Boothroyd, G. and Knoght, W. A., *Fundamentals of Machining and machine Tools*. New York Marcel Dekker, Inc., 1989.

[26] Reshetov, D. N. and Protman, V. T., *Accuracy of Machine Tools*. ASME Press, New York, 1988.